Managing Multihoming Workers in the Gig Economy

Gad Allon
The Wharton School, University of Pennsylvania, Philadelphia, PA 19104
gadallon@wharton.upenn.edu

Maxime C. Cohen
Desautels Faculty of Management, McGill University, Montreal, QC H3A 1G5, Canada
maxime.cohen@mcgill.ca

Ken Moon
Cornell SC Johnson College of Business, Cornell University, Ithaca, NY 14853
kenmoon@cornell.edu

Wichinpong Park Sinchaisri
Haas School of Business, University of California, Berkeley, CA 94720
parksinchaisri@haas.berkeley.edu

February 18, 2026

Abstract. Gig economy platforms increasingly compete to source labor from common pools of multihoming workers, who dynamically allocate their services between competing platforms. Therefore, the question of how platforms can design pay and other levers to attract labor has gained significance. However, standard gig economy data are often incomplete from a choice modeling perspective, which impedes platforms' understanding of workers' multihoming preferences and choices. We study this problem using data shared by a major ride-hailing platform integrated with public data revealing the drivers' outside options in NYC. We structurally estimate a dynamic work-or-switch model using a novel combination of simulation and adversarial machine learning to overcome the empirical problem of contextually incomplete choice data. We find drivers to be significantly focused on short-horizon intraday payoffs while displaying significant heterogeneity in their costs of working. We offer prescriptions for platforms based on counterfactual analyses. We find that at a fixed labor cost, offering dynamic but guaranteed hourly pay rates can increase labor capacity over paying workers on a per-trip basis. A substantial segment of drivers are rarely observed to use pay-per-work platforms and would demand substantially increased compensation to accept that mode of pay. Next, we conduct a counterfactual policy exercise based on New York City's Driver Income Rules; this out-of-sample exercise validates recent empirical studies showing that higher posted pay worsens congestion while achieving muted gains in realized earnings. As alternative levers, platforms can reduce multihoming via offering streak bonuses, but impeding quits induces drivers to switch earlier to other platforms. Overall, managing multihoming requires aligning pay timing with workers' decision horizons, and instituting wage floors requires complementary measures to manage increased congestion.

Key words: Gig economy, Incentives, Multihoming, Structural estimation, Applied generative adversarial networks, Empirical operations, Behavioral operations

1. Introduction

The gig economy places platforms in competition for on-demand workers, who prevalently "multihome" by choosing flexibly for which provider to work. Not just daily but continually throughout the day, these workers dynamically allocate their labor supply across various platforms in real-time. Illustratively, many ride-hailing drivers use multiple platforms to find and complete both rides and

food deliveries. In fact, approximately 39% of U.S. gig workers actively worked two or more types of gigs in 2021, increasing substantially from 14% in 2016 (Anderson et al. 2021)

For platforms, the challenge of managing a multihoming workforce has only grown. Cities including New York City (NYC) and Seattle have capped the total number of drivers eligible to work in the ride-hailing sector in response to mounting traffic congestion and concerns for driver welfare (Fitzsimmons 2018, Wilson 2019). Such market conditions generate fierce competition among platforms for a limited pool of multihoming gig workers, and as the competition stiffens, gig workers often dedicate smaller shares of their time and labor to any single platform.

As multihoming becomes a more central concern, platforms are compelled to optimize their use of levers to attract and deploy their labor supply. These levers span from the financial, in terms of the structure and amount of compensation paid to drivers, to the operational, such as the availability of jobs and the selection offered. Because platforms as firms must understand how drivers react to their management of these levers, firms must additionally understand and work around the shortcomings of their own data in fully capturing drivers' choices and reactions.

In this study, we focus on a gig platform's use of financial pay incentives, operational levers, and proprietary data in managing a multihoming workforce. In terms of levers, we focus most heavily on the empirical study and optimization of driver pay. Traditionally, the conventional model of platform operations relies primarily on flexible wages (e.g., surge prices) paid in *pay-per-work* schemes in order to clear a platform's own market (Chen et al. 2019). For instance, Uber compensates drivers for each trip they complete, at dynamic wages that depend on the time and distance, traffic conditions, and the current ratio of drivers over rider demand. However, as platforms proliferate and a limited number of drivers participate in numerous marketplaces at once, platforms' pay structures must adapt. Beyond immediately clearing their own spot markets, platforms must offer drivers workflows and compensation schemes that remain appealing in the face of competing offers.

Using real-world data from NYC, we examine the need for a platform to consider broader pay schemes for gig work in the presence of platform competition and workers' ability to multihome. In particular, inspired by the innovative pay scheme of our collaborating platform, a major ride-hailing platform operating in NYC, we study the effects of committing to a guaranteed pay schedule in advance. Under this pay scheme, the platform still experiences fluctuations in market demand but resolves to absorb such demand uncertainty itself in favor of preannouncing to its drivers dynamic hourly pay rates set in advance. Beyond our empirical examination of such steadier pay, we examine

whether operational levers can, as an alternative, offer platforms the same advantages in managing drivers' choices.

A major component of our paper concerns the realistic limitations of the proprietary data available to modern gig platforms. Whereas gig platforms operate in a highly data-intensive fashion, they collect and maintain data with business and engineering priorities in mind. As a result, their proprietary data regularly omit details relevant to understanding the full context of drivers' choices, and such omissions are commonly faced in the broader literature. For instance, retailers and retail platforms predominantly *fail* to report minute to minute changes in *offered* product details, such as prices, in their data. Instead, both retailers and researchers rely on scanner or point-of-sale data that record extensive product details, such as the exact offered price, only when transactions occur. As a result, it is commonplace in the marketing, operations, and economics literature to impute the prices of competing but *unchosen* products based on surrounding but inexact transactional data. That is, firms widely engage in *event-driven* data capture, in which many precise details are only kept and reported upon the occurrence of an event of interest, such as a product's actual purchase.

However, every choice is made within a surrounding context that includes the prices and attributes of other products. An unbiased choice analysis would ideally rely on the availability of detailed data regarding all choices at all times, including even for choices of no purchase. Like retailers, gig economy platforms prevalently capture event-driven data, rather than data intended to capture the full context of all choices. With relevance to us, for example, our collaborating platform logged data regarding the exact circumstances faced by drivers when they terminate a workshift on the platform but did not do the same for every mid-shift moment when the same drivers chose *not* to terminate. In light of the scale and complexity of their operations, ridehailing platforms frequently engage in event-driven data capture surrounding driver behavior of interest.

This problem of missing context for choices is widespread in industry practice, but we argue that it is more consequential for studying choices in the gig economy than for retail. An observed choice about how to work right now depends not only on missing context now but also on missing context about the future. The effect of unobserved contexts compounds dynamically.

Our study addresses three primary research questions: (i) How do multihoming gig economy workers evaluate the dynamic and potentially uncertain evolution of a platform's available work opportunities and pay? Ultimately, their evaluations shape the platform's labor supply. (ii) How can choice estimation methodology overcome the missing context problem that widely affects

proprietary industry data? (iii) Lastly, how should gig platforms optimize their pay schemes in light of our empirical findings? We also consider operational substitutes for restructuring pay.

Using data shared by a major ride-hailing platform based in NYC, we structurally model and estimate ride-hailing drivers' preferences for work and pay. Specifically, the model explains each driver's dynamic decision-making on the basis of her detailed time and location, the on-platform pay she is offered, and the availability and pay of the main competing platform.

We estimate the structural model using novel indirect inference methods that combine simulation with machine learning (Gourieroux et al. 1993, Kaji et al. 2023). Whereas these methods have previously been used to recover preferences from highly complex choice sets (Moon 2023),we show how these methods can address the missing context problem in data-driven settings where choice environments are only partially observed.

We first recognize that the missing context problem amounts to a form of biased censoring of choice data under which the *choice outcome* determines the visibility of the *explanatory variables*. Our methodology overcomes this selection bias by leveraging the structural model and broader aggregate data to fill in the implicit missing context. In our setting, we source unbiased data regarding aggregate choices from the public corpus of all NYC ride-hailing trips kept by the Taxi and Limousine Commission (TLC). Researchers can view our approach, which utilizes machine learning and simulation of the structural model to match proprietary and aggregate outcomes, as an extension of the practice of imputing product prices from surrounding datapoints when a product's exact price is only observed when actually purchased in scanner or point-of-sale data.

Using these methods, our structural empirical framework recovers drivers' discount factors and costs of working. We especially find that drivers strongly discount their future earnings. Because they then focus heavily on immediate earnings, they frequently multihome between platforms—with 66.59% of the drivers on our studied platform switching between platforms on more days than not. Despite this, we find that the platform's steady pay rates greatly reduce the frequency of drivers' switching between platforms—that is, they would choose to switch even more frequently if the platform's pay rates were variable. In particular, offering guaranteed wages allays switching because drivers know that they can anticipate steady wages in the short-term future, whereas highly variable wages are subject to uncertain and rapid fluctuations. Our counterfactual analyses show that guaranteed wages offer platforms a more cost-effective path to a stable labor supply.

Secondly, we find that rewarding drivers with compensatory bonuses for "streaks" or for completing all assigned offers within a pre-allotted time frame similarly discourages multihoming. In

contrast, measures that operationally impede workers from quitting the platform can backfire by motivating workers to switch earlier in anticipation.

Finally, we use our estimated model to study NYC's 2018 *Driver Income Rules*, which imposed minimum wage standards on ride-hailing platforms, and we show how wage regulation can have unintended consequences for multihoming workers when it interacts with platform pay design and dynamic switching incentives.

1.1. Related Literature

Our study builds on a growing operations management literature on gig economy platforms and on-demand labor supply (see Benjaafar and Hu 2020). A central insight of this work is that platforms use flexible work arrangements to cope with demand uncertainty, but that this flexibility shifts key operational decisions to workers, including when to be available and which opportunities to pursue. Early analytical models clarify how platforms can use compensation and matching levers to manage supply in such decentralized settings (e.g., Ibrahim 2018, Dong and Ibrahim 2020, Besbes et al. 2021, Benjaafar et al. 2022), and related work argues that flexible contracting can be operationally advantageous relative to employment when demand is volatile (Lobel et al. 2024). Motivated by these foundations, we focus on pay design in a setting where labor supply is contestable because workers can switch across platforms within the day.

Empirically, evidence suggests that workers respond to compensation in ways that go beyond a spot-market view. Miao et al. (2022) leverage a quasi-experiment around surge pricing and show that dynamic pay changes who works and when, with heterogeneous responses across driver types. Allon et al. (2023) similarly finds that drivers respond not only to the monetary value of incentives but also to internal goals and reference points. From a labor-economics perspective, Mas and Pallais (2017) quantify workers' willingness to pay for alternative work arrangements, highlighting how predictability and flexibility are valued job attributes. Together, these findings motivate our premise: in competitive markets with multihoming, a platform's pay policy shapes not only how much labor it attracts, but also how reliably it retains workers' attention as outside opportunities fluctuate.

A second stream relates to multihoming and platform competition. Prior work documents multihoming on the consumer side, where users compare options before committing (Critero 2017, Davies et al. 2022), and in advertising markets, where multihoming can affect match efficiency and equilibrium prices (e.g., Athey et al. 2018, Park et al. 2021). On the provider side outside gig work, multihoming has been linked to frictions and adaptation costs, such as developers porting products across platforms (Landsman and Stremersch 2011, Cennamo et al. 2018). These studies establish

multihoming as a general feature of platform competition, but they do not capture what makes gig work operationally distinctive: switching can occur at high frequency, with immediate implications for utilization, waiting time, and earnings, and with platform levers that evolve dynamically throughout the day.

In the gig economy, both consumers and providers can multihome, but provider-side multihoming is especially consequential because it is the mechanism through which competition reshapes effective labor supply. On the consumer side, Chitla et al. (2023) models riders' platform choice with potential loyalty effects. On the worker side, theory suggests that multihoming can reduce idle time by expanding the set of available jobs (Bryan and Gans 2019, Loginova et al. 2022). At the same time, equilibrium analyses caution that multihoming can lower earnings or welfare once platforms react strategically (Benjaafar et al. 2020, Bernstein et al. 2021), and Tadepalli and Gupta (2020) argues that it may induce inefficient platform policies with long-run consequences. Despite these predictions, cross-platform worker multihoming remains difficult to measure empirically at high frequency, and we still lack clear evidence on which levers reliably influence workers' switching decisions in the field when pay and availability evolve stochastically in real time.

Our paper addresses this gap by structurally modeling and empirically estimating worker multihoming in a large, competitive ride-hailing market. Closest to our work are Rosaia (2025) and Allon et al. (2025). Rosaia (2025) studies competing platforms using high-frequency NYC data with a focus on allocation, pricing, and congestion-related interventions. We complement this perspective by focusing on policies designed to influence switching incentives and by quantifying how alternative pay schemes affect multihoming. Allon et al. (2025) measures multihoming and repositioning using proprietary driver analytics data and evaluates policies intended to limit multihoming or congestion. In contrast, we focus on multihoming as the primary behavioral margin and study in depth the competing pay schemes that are central in practice, while also evaluating monetary and non-monetary substitutes, including streak-style bonuses and operational frictions.

Finally, our counterfactual analyses speak to a broader literature on incentive design for gig platforms and regulators. While pay-per-task remains prevalent, guaranteed pay schemes have emerged in practice (e.g., Browning 2023), raising a basic but unresolved question: when does income certainty reduce switching, and at what cost? Stability is widely valued by gig workers (Chen et al. 2019), and even with flexibility, many workers maintain regular patterns of work and platform engagement (Allon et al. 2023). Beyond the gig economy, evidence suggests that pay variability can increase turnover and reduce motivation and completion (Ikeda and Bernstein 2016,

Cameron and Meuris 2022, Butschek et al. 2022). At the same time, wage-based incentives can be inefficient when they intensify competition or fail to address worker heterogeneity (Chen et al. 2022, Besbes et al. 2022). Complementing monetary levers, recent work shows that non-monetary interventions can meaningfully shape behavior, including feedback (Bolton et al. 2004, Athey et al. 2024), relative rankings (Choudhary et al. 2022, Shokoohyar and Katok 2022), information design (Li and Zhu 2021), and priority matching (Mai et al. 2023). Our analyses characterize when income certainty and engagement-contingent rewards can discourage multihoming, and when operational frictions can backfire once workers anticipate future switching opportunities.

1.2. Methodological Contributions

A major contribution of this paper is methodological. In many data-driven environments, rich state information is recorded at salient events but not at non-events, even though non-events are precisely when agents reveal that they preferred to continue rather than exit. In our setting, the focal platform logs detailed context at session start and termination but not at intermediate decision epochs when drivers continue working. This outcome-dependent observability makes it difficult to apply standard dynamic discrete choice methods that condition on per-epoch states, because the states are selectively observed.

We develop a structural estimation approach that leverages outcomes that are observed consistently, rather than conditioning on selectively observed states. We combine a dynamic model of within-day stay, switch, and quit decisions with simulation-based estimation (Gourieroux et al. 1993, Pakes and Pollard 1989) and adversarial objectives (Kaji et al. 2023), using high-dimensional spatial-temporal quitting patterns as the target outcomes. Conceptually, the missing-context challenge parallels environments in which relevant alternatives are only imperfectly observed through attention or information acquisition (Goeree 2008, Cattaneo et al. 2020). In our application, the approach also requires bringing the outside market into the state: we construct a time-varying measure of outside opportunities from public records using neighborhood-by-hour imbalances between nearby pickups and drop-offs, which allows us to interpret departures as revealed responses to competing opportunities and to conduct counterfactuals with proprietary data from the focal platform plus public records.

Substantively, our estimates quantify short planning horizons over within-day decisions and substantial heterogeneity in perceived costs of working, which together rationalize frequent within-day reallocation across platforms. These estimated primitives discipline counterfactuals that speak directly to platform design and regulation under multihoming: when guaranteed pay retains capacity

relative to pay-per-work at comparable expected earnings, when streak-style bonuses reduce multihoming, and when operational frictions that delay exit can backfire by inducing earlier switching in anticipation of being locked in during unattractive future states. Many of these points are developed in the introduction and then made precise in the estimation approach (§4) and the counterfactual analysis (§6).

2. Setting and Data: Ride-hailing Work Sessions in New York City

We study ride-hailing labor supply in NYC, where multiple platforms operate side by side, and drivers choose throughout the day whether to continue working on a given platform or reallocate their time elsewhere. This setting is central to our research questions, but immediately raises a measurement challenge: we observe rich behavior on our focal platform yet do not directly observe the full menu of outside opportunities a driver faced at every moment. Our approach pairs proprietary session-level data from a U.S. ride-hailing platform (platform *A*) with NYC's public trip records from the TLC, which provide high-frequency, market-wide information on ride-hailing activity across platforms. Together, these data allow us to measure drivers' session start and end decisions on platform *A* and to construct time- and location-varying proxies for the strength of outside opportunities.

2.1. Proprietary Data from Platform *A*

Platform *A* operates in several U.S. cities. We focus on NYC because it allows us to pair the proprietary driver-session records with comprehensive public data on ride-hailing activity and competition. The platform mainly offers shared rides, and the majority of its customers are regular commuters with relatively consistent demand for work commutes and a need for reliable service.

Drivers on platform *A* are compensated at a guaranteed hourly wage rate, conditional on remaining online and following the navigation instructions supplied by the platform.[1] Hourly rates, referred to as *offers*, are set at the granularity of day of week and time interval within each day and are communicated in advance through text messages.

A *shift* refers to a time interval during which the hourly offer rate is fixed. The shifts are as follows: morning rush hours from 7 to 9 a.m. *(AM peak)*, from 9 a.m. to 5 p.m. *(midday)*, afternoon rush hours from 5 to 8 p.m. *(PM peak)*, evening non-rush hours from 8 to 9 p.m. *(PM off-peak)*, and from 9 p.m. to midnight *(late night)*. Drivers do not need to work an entire shift's duration;

[1] When not matched with passengers, drivers are instructed to relocate to specific locations and their real-time location is tracked by GPS to confirm that they are still working for the platform.

instead, they are paid pro rata at the offer rate times the actual time they work (that is, are online and following navigation instructions). Most rides are shared by multiple passengers, and the platform utilizes its drivers at higher rates than other ride-hailing platforms. Consequently, drivers rarely relocate independently, supporting our simplifying assumption that drivers remain in their current regions when not matched with passengers.

We leverage two sets of proprietary data from platform A for their NYC operations in July 2017. The first dataset contains, for every driver's active shift, information on her driving activities and financial incentives including offers. The data include each driver's anonymized ID and vehicle type, her experience with the platform, the duration she worked during the shift, and the shift's hourly offer rate. We merge these with a second dataset that reports, for every work session, the driver's first pick-up and last drop-off. A work session is defined as an uninterrupted span of time during which the driver remains actively logged into the platform. For each session, we observe the driver ID and the exact timestamps and GPS coordinates of the driver's first and last trips. In total, these data cover 45,208 work sessions performed by 2,875 drivers.

2.2. Public TLC Trip Records and Market-Wide Conditions

We also leverage public trip-record data collected by NYC's Taxi and Limousine Commission (TLC), which reports the pick-up and drop-off location and time for every ride-hailing trip taken in the city across all platforms.[2] For each trip, we observe timestamps, neighborhood-level pick-up and drop-off locations, and the dispatching base, which we use to identify the platform operating the trip. We cannot identify or trace individual drivers across trips.

We use the TLC data for two purposes. First, we use trip-level information to approximate the path taken by each active driver on platform A during each work session. Because the proprietary data from platform A report only the first pick-up and last drop-off of each session, we use the TLC dataset to estimate origin-destination transition probabilities conditional on location and time. These transition probabilities allow us to reconstruct the likely sequence of locations visited by a driver who starts a session at a given origin and time and then receives a sequence of trips on A.

Second, we use the TLC data to construct time- and location-varying measures of outside opportunities on competing platforms. During our sample period in summer 2017, four major ride-hailing platforms operated in NYC, including our industry partner. In the model, we summarize the outside option using the largest competing platform, which we refer to as platform B. Ride-hailing

[2] See https://www1.nyc.gov/site/tlc/about/tlc-trip-record-data.page.

trip volumes were highly concentrated among a small number of large firms. We therefore treat platform B as a representative outside ride-hailing platform and interpret the outside-option index constructed from B's trip records as a lower bound on the value of all ride-hailing alternatives available at a given time and location.[3] From the TLC records, we obtain, by location and time, the number of completed trips on B, the distribution of trip durations, and empirical transition probabilities for destinations. We then augment these data with trip fares calculated using publicly posted, duration- and distance-based pricing formulas. Together, these pieces allow us to construct, for each neighborhood and decision epoch, an estimate of the expected earnings available on B.

2.2.1. Proxying for outside options. Because our empirical framework relies on short-run movements in the relative attractiveness of A versus B, we construct a high-frequency index of supply shortage on B, which we interpret as a proxy for surge-style pay and hence for the outside-option value drivers anticipate on B. Intuitively, we look for situations in which many trips *start* on B in a neighborhood and hour even though relatively few trips *end* there in the same period. In such cases, the number of B pick-ups exceeds the number of local drop-offs that could have supplied drivers to that neighborhood. The extra pick-ups must then be served by drivers who repositioned into the neighborhood from elsewhere, which is consistent with stronger incentives or better immediate opportunities on B.

Formally, for each neighborhood l and decision epoch t, we compute:

$$\text{Shortage}^B_{lt} \equiv \max\{\text{Pickups}^B_{lt} - \text{Dropoffs}^B_{lt}, 0\},$$

where Pickups^B_{lt} and Dropoffs^B_{lt} denote the number of trips on B that pick up from, and drop off in, neighborhood l during epoch t. We combine Shortage^B_{lt} with the imputed expected trip earnings to obtain a measure of outside-option value that varies both over time and across neighborhoods. Appendix A.1 provides additional details and validation of this construction.

2.3. Descriptive Patterns on Platform A

The proprietary data reveal several key empirical patterns about how drivers work under guaranteed hourly wages in a competitive market. These patterns inform our modeling choices and highlight the within-day switching decisions that are central to platform competition for multihoming workers.

[3] We do not observe where drivers go after leaving platform A: they may switch to B, switch to a smaller platform, take a different type of job, or quit working for the day. Our identification strategy does not require labeling each exit. Instead, it relies on associating exits with temporal and spatial variation in B's attractiveness. When our outside-option proxy for B spikes in a specific neighborhood and hour, we see a corresponding increase in exits from A, which disciplines the switching margin even though the exact destination is unobserved (see Appendix A.1 for details).

Most drivers work single, uninterrupted shifts per day. The typical driver completes one long work session per day rather than multiple short sessions. The average driver works 1.33 sessions per day (median 1.24), with session durations averaging 4.50 hours (median 3.03 hours). Conditional on working, drivers accumulate 6.34 daily hours on platform A (median 5.55 hours). The time between consecutive sessions averages 36.83 hours (median 12.51 hours), confirming that drivers typically return on different days rather than taking brief breaks within a day. This concentration into single daily sessions indicates that once drivers begin work, they make a sequence of short-horizon decisions about whether to continue, switch platforms, or quit for the day.

Drivers do not work overnight and rarely return after leaving. Nearly all sessions (91.86%) start and end on the same calendar day. Figure 1 shows when drivers start and end their sessions. Starts cluster sharply at shift boundaries (7am, 9am, 5pm), while endings concentrate around the conclusion of peak wage periods (9am, 5pm, 8pm). Between these times, starts and ends are relatively sparse. Combined with the low rate of multiple same-day sessions, this pattern indicates that the decision to leave platform A is effectively terminal for that day; drivers who exit do not return. This motivates our modeling assumption that switching from platform A to competing platform B is absorbing within the workday.

Figure 1 Distributions of the hours of the first and last trips in drivers' work sessions

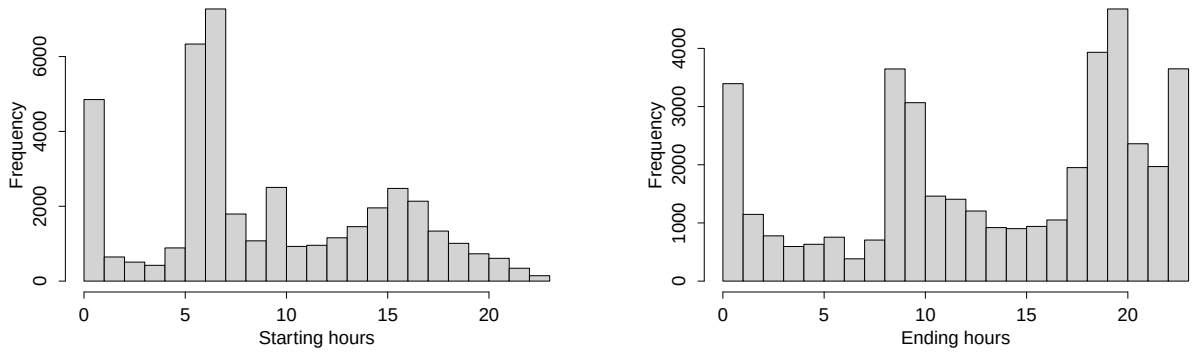

(a) Hour of the first trip in the session

(b) Hour of the last trip in the sessions

Note: Session starts cluster at shift boundaries when wages change. Endings concentrate when high-wage periods conclude.

Guaranteed wages vary substantially across shifts, and drivers time their work accordingly. Platform A preannounces guaranteed hourly wages that differ by shift, day of week, and individual driver. Figure 2 shows the distribution of offered wages by shift. On weekdays, morning rush hours (7–9am) command median wages of \$40–\$45 per hour, midday offers \$35–\$40, and evening wages decline to \$30–\$35. Weekend wages are somewhat lower but follow a similar peak-midday-evening

gradient. The fact that session starts and ends cluster precisely at shift boundaries suggests that drivers actively respond to this wage schedule. They time market entry to capture high-wage shifts and consider exiting when wages decline, even though wages remain well above market alternatives.

Figure 2 Hourly guaranteed wage rates offered to drivers, by shift

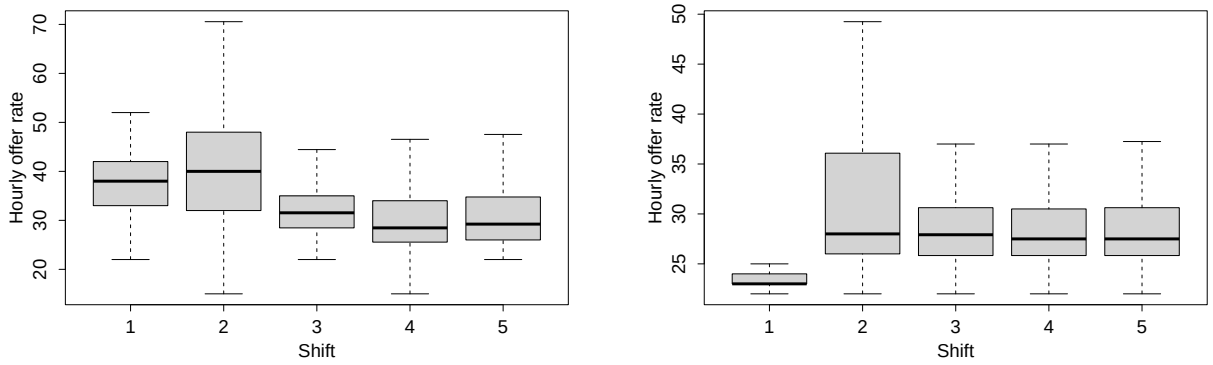

(a) Weekdays (b) Weekends

Note: Shifts from 1 to 5 are morning rush (7-9am), midday (9am-5pm), afternoon rush (5-8pm), evening (8-9pm), and late night (9pm-12am). Higher wages during rush hours reflect demand patterns.

Despite high earnings, drivers remain responsive to wage changes. Daily earnings average $230.90 (median $211.35), as shown in Figure 3. The implied hourly earnings rate of $36.42 is more than three times NYC's 2017 minimum wage of $11.00. Yet even at these wage levels, drivers do not exhibit perfect loyalty to platform A. The clustering of session endings at shift boundaries when wages change suggests that well-compensated drivers continue to compare platform A's current offer to outside opportunities and may switch when relative pay conditions shift. This pattern raises the central question for our analysis: how should platforms design compensation to retain multihoming workers who can reallocate quickly to competitors?

Drivers traverse neighborhoods during shifts, creating spatial variation in opportunities. While most drivers remain within a borough during their shift (74.62% of sessions start and end in the same borough), they traverse multiple neighborhoods as trips unfold. Only 2.06% of sessions start and end in the same neighborhood. This mobility matters because both platform A's matching conditions and the attractiveness of competing platform B vary across neighborhoods and over time. A driver's current location determines her immediate matching probability on A as well as the strength of outside opportunities, which we construct from public TLC data as described in Section 2.2.1.

Figure 3 Daily work outcomes conditional on working

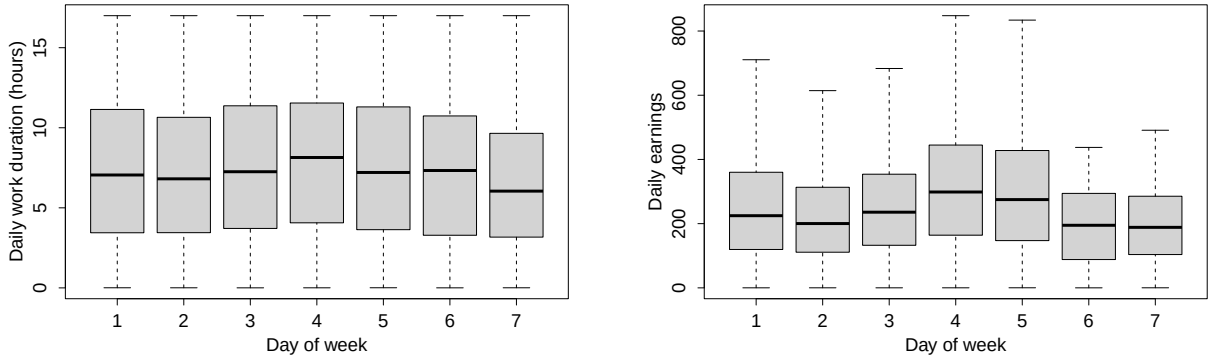

(a) Daily work duration (hours)

(b) Daily earnings

Note: Substantial variation across days of the week reflects both demand patterns and the guaranteed wage structure.

These patterns jointly inform our modeling approach. We study drivers who make within-day decisions about whether to continue working on platform A, switch to a competing platform, or quit for the day. The decisions unfold over short time horizons (drivers cluster work into single sessions and respond immediately to wage changes at shift boundaries), exits are effectively absorbing (drivers who leave do not return that day), and the choice environment varies over both time and space. The next section formalizes this decision problem.

3. Model of Gig Platforms and Worker Decisions

We formalize multihoming in a ride-hailing market where drivers can reallocate their time across platforms within the day. Two platforms operate in the same city and provide comparable ride-hailing service, but compensate drivers differently. Platform A (our focal platform) offers a guaranteed hourly wage while a driver remains logged in and available. Platform B (the main competing outside option in our model) pays per trip, with compensation varying with trip conditions. This contrast is central to our analysis: guaranteed hourly pay provides income certainty but commits the platform to absorbing demand fluctuations, whereas per-trip pay shifts more earnings variability to drivers but pays only when work is realized.

Drivers revisit the where-to-work decision throughout the day. When they become available between trips (or after an idle interval), they decide whether to remain on their current platform, switch, or stop working for the day. These decisions depend on both time and location, platform-specific pay and matching conditions, and drivers' heterogeneous costs of working and forward-looking tradeoffs.

3.1. Market Structure and Timing

The market is defined over L regions and covers trips that originate and end within the city. We discretize service hours into 20-minute decision epochs, indexed by t, reflecting the average ride-hailing trip duration. Drivers do not abandon customers mid-ride. Between rides (or after an idle epoch), a driver chooses whether to continue working and, if on A, whether to switch platforms.

We focus on platform A's ability to retain drivers once they have joined. Consider a driver located in region l at epoch t. On platform A, she is matched with probability R^A_{lt}. If matched, her destination is k with probability π^A_{lkt} and the ride lasts τ^A_{lk} epochs. We assume drivers accept matches. If unmatched, she remains in region l through the epoch and revisits her decision at $t+1$.

Timing of compensation during trips. When a driver on platform A is matched at the start of epoch t, she earns the guaranteed wage rate $w_{it}/3$ per epoch for all epochs spanned by the trip. Critically, the wage rate w_{it} is determined at the trip start and remains constant throughout the trip duration, even if the trip spans multiple epochs. This reflects platform A's practice of pre-announcing wages by shift, with trips designed to complete before shift boundaries. On platform B, the driver receives fare f^B_{lkt} upon trip completion (modeled as paid at the end of epoch $t+\tau^B_{lk}-1$). In both cases, the driver incurs per-epoch cost C_i during all active epochs, whether matched or idle.

If the driver switches from A to B, she faces an analogous environment on B, with match probability R^B_{lt}, destination probabilities π^B_{lkt}, and trip durations τ^B_{lk}. Empirically, drivers rarely work multiple disjoint sessions on the same platform within a day, so we treat switching as absorbing within-day: a driver who switches from A to B does not return to A that day. Figure 4 summarizes the decision flow.

3.2. Worker Preferences

We model drivers as forward-looking decision-makers who differ in their willingness to continue working under given pay conditions. This heterogeneity arises from differences in costs: drivers face different opportunity costs, effort tolerances, and outside options, while all drivers share a common planning horizon over within-day decisions. This specification captures our setting well and, critically, aligns with what our data can identify.

Our approach utilizes a forward-looking discount factor rather than attempting to separately estimate risk aversion parameters. Here is why this matters: with data on within-day work durations and exit decisions but not on consumption, wealth, or direct risk elicitation, the discount factor β is substantially better identified than a separate risk aversion parameter. Both parameters affect choices in similar ways; they both make drivers more willing to accept lower current pay for future

Figure 4 Model overview

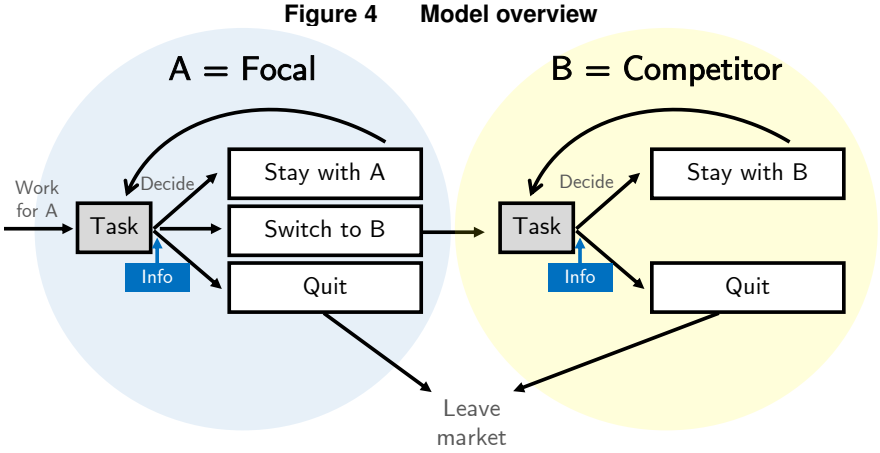

Note: A driver starts on platform A and, when available between trips, decides whether to stay on A, switch to B, or quit for the day. After switching to B, she decides whether to stay on B or quit.

rewards, and even controlled experimental designs struggle to separately identify them without dedicated instruments (Andersen et al. 2014). We therefore treat utility as linear in earnings and interpret β as a reduced-form measure of effective planning horizon. Under this interpretation, the cost parameter C_i bundles opportunity costs, effort and fatigue, and any disutility associated with earnings variability.

More generally, while present-biased or heterogeneous discounting can matter in principle (Laibson 1997, O'donoghue and Rabin 1999), our parsimonious specification is designed to match the multihoming and quitting behavior we observe while remaining credibly identified by our data.

Driver i has an average per-epoch cost C_i drawn from a truncated Normal distribution with mean μ_C and variance σ_C^2 over support $[\underline{C}, \bar{C}]$. In each decision epoch, the driver also receives action-specific i.i.d. Type I extreme value shocks $\{\epsilon^a_{ilt}\}$, which capture unobserved factors affecting stay, switch, and quit decisions. All drivers share a common exponential discount factor $\beta \in (0,1)$ applied to each 20-minute epoch.

3.3. Work Decisions on Platform A

A driver i available on platform A at location l and time t chooses among {stay on A, switch to B, quit}. While active on A, she earns a guaranteed hourly wage w_{it}, which translates to $w_{it}/3$ per epoch, whether matched or idle. Quitting yields value normalized to zero.

Let $V_i(\text{Stay}; A, l, t)$ denote the expected discounted value of staying on A from the start of epoch t, excluding the action-specific shock $\epsilon^{\text{Stay}}_{ilt}$. Following the timing convention above, the driver first receives flow payoff $(w_{it}/3 - C_i)$ during epoch t. With probability $1 - R^A_{lt}$, she remains unmatched; in

this case, epoch t passes while she waits, and at the start of epoch $t+1$ she makes a new decision with continuation value $V_i^*(A, l, t+1)$. With probability R_{lt}^A, she is matched with a customer. Conditional on matching, destination k occurs with probability π_{lkt}^A, the trip lasts τ_{lk}^A epochs (deterministic), and the driver earns $(w_{it}/3 - C_i)$ during each of these τ_{lk}^A epochs. At the start of epoch $t + \tau_{lk}^A$, she arrives at location k and makes a new decision with continuation value $V_i^*(A, k, t + \tau_{lk}^A)$.

Combining these cases:

$$V_i(\text{Stay}; A, l, t) = \left(\frac{w_{it}}{3} - C_i\right) + (1 - R_{lt}^A) \cdot \beta V_i^*(A, l, t+1) + R_{lt}^A \cdot \sum_{k=1}^{L} \pi_{lkt}^A \left[\left(\sum_{s=1}^{\tau_{lk}^A - 1} \beta^s \left(\frac{w_{it}}{3} - C_i\right)\right) + \beta^{\tau_{lk}^A} V_i^*(A, k, t + \tau_{lk}^A)\right], \tag{1}$$

where the inner sum runs from $s = 1$ to $\tau_{lk}^A - 1$ because the first epoch's flow payoff is already included in the leading term $(w_{it}/3 - C_i)$.

Switching from A to B yields the value of beginning the epoch on B at the same state:

$$V_i(\text{Switch}; A, l, t) = V_i(\text{Stay}; B, l, t), \qquad V_i(\text{Quit}; A, l, t) = 0.$$

With Type I extreme value shocks, the continuation value on A is the inclusive value

$$V_i^*(A, l, t) = \log\left(\exp(V_i(\text{Stay}; A, l, t)) + \exp(V_i(\text{Switch}; A, l, t)) + \exp(0)\right). \tag{2}$$

3.4. Work Decisions on Platform B

A driver available on platform B at location l and time t chooses between staying and quitting. If she stays, she matches with probability R_{lt}^B. Conditional on a match, her destination is k with probability π_{lkt}^B, the ride lasts τ_{lk}^B epochs (deterministic), and she receives expected fare f_{lkt}^B paid at trip completion (end of epoch $t + \tau_{lk}^B - 1$). If unmatched, she remains in l, pays cost C_i during epoch t, and revisits her decision at $t+1$. Quitting yields value normalized to zero.

The expected discounted value of staying on B is:

$$V_i(\text{Stay}; B, l, t) = (-C_i) + (1 - R_{lt}^B) \cdot \beta V_i^*(B, l, t+1) + R_{lt}^B \cdot \sum_{k=1}^{L} \pi_{lkt}^B \left[\left(\sum_{s=1}^{\tau_{lk}^B - 1} \beta^s (-C_i)\right) + \beta^{\tau_{lk}^B} \left(f_{lkt}^B + V_i^*(B, k, t + \tau_{lk}^B)\right)\right], \tag{3}$$

where the fare f_{lkt}^B is received at the end of the trip (modeled as occurring at the start of epoch $t + \tau_{lk}^B$ in discounted terms), and the continuation value follows.

The inclusive value on B is:

$$V_i^*(B, l, t) = \log\left(\exp(V_i(\text{Stay}; B, l, t)) + \exp(0)\right). \tag{4}$$

This model generates within-day sequences of stay, switch, and quit decisions as a function of time, location, and the evolving attractiveness of work on A versus outside opportunities summarized by B. In the next section, we describe how we construct the objects $\{R^A, \pi^A, \tau^A, w\}$ and $\{R^B, \pi^B, \tau^B, f^B\}$ from the proprietary and TLC data, and how we estimate (β, μ_C, σ_C) by matching simulated and observed patterns of session terminations on A.

4. Estimation Strategy and Implementation

Standard dynamic discrete choice estimation typically assumes that we observe the relevant state at each decision point. As discussed in §1-2, our proprietary data violate this assumption in a systematic way: platform A logs rich context when a work session starts or terminates, but not at each intermediate epoch when a driver chooses to continue. This outcome-dependent observability means that we cannot derive a likelihood for each driver's decisions as a function of the full state.

We address this challenge using adversarial estimation (Kaji et al. 2023). Rather than condition on selectively observed states, we estimate preference parameters by matching the distribution of high-dimensional quitting outcomes that remain well defined and consistently observed at the day level. Intuitively, we simulate driver trajectories under the structural model and choose parameters so that simulated quitting patterns are indistinguishable from those observed in the data.

4.1. Adversarial Estimation

Two natural approaches to estimating our model both break down under outcome-dependent observability. Maximum likelihood estimation would require observing the complete state at every decision point, allowing us to express the probability of observed choices conditional on observed states. Here, however, the states we observe are precisely those at which drivers chose to begin or quit their session on platform A. Conditioning on observed states would introduce selection bias because quitting determines observability. The states we observe are precisely those where drivers chose to exit, not a representative sample of all states encountered.

A second approach is indirect inference with a small set of hand-selected moments, matching aggregate statistics rather than individual choice probabilities. For example, one could match the mean quit time, the share of drivers who leave during peak hours, or the overall spatial dispersion of quits. The difficulty is that quitting patterns in our setting are intrinsically high-dimensional (e.g., possible times and locations). Reducing these patterns to a few scalar moments

risks discarding information that is important for separating forward-looking from myopic behavior and for distinguishing high-cost from low-cost drivers.

Adversarial estimation automates the selection and weighting of informative features of the data through machine learning (Kaji et al. 2023). Rather than pre-specifying moments, we train a discriminator, generally a neural network, to distinguish the observed quitting outcomes from outcomes simulated by the structural model. We then search for preference parameters that make this classification task as difficult as possible. When the discriminator cannot reliably tell simulated from observed outcomes, the model has captured the mapping from incentives and outside options to quitting behavior that is present in the data.

Formally, let X denote observed daily outcomes and let X^θ denote simulated daily outcomes generated under preference parameters $\theta = (\beta, \mu_C, \sigma_C)$. A discriminator $D : \mathcal{X} \to [0,1]$ maps an outcome to the probability that it comes from the observed data rather than the simulation. We solve the minimax problem

$$\min_{\theta} \max_{D \in \mathcal{D}} \mathbb{E}[\log D(X)] + \mathbb{E}\Big[\log\Big(1 - D(X^\theta)\Big)\Big], \tag{5}$$

where $\mathcal{D}$ is a class of feed-forward neural networks. The inner maximization trains the discriminator to classify real versus simulated outcomes, while the outer minimization updates θ so as to reduce the discriminator's ability to do so. This minimax structure is closely related to generative adversarial networks (Goodfellow et al. 2014). Under regularity conditions, Kaji et al. (2023) show that this adversarial estimator is consistent and asymptotically normal; Appendix B.1 verifies that our implementation satisfies their assumptions.

Resolving the missing context. The key is that we do not need to evaluate per-epoch choice probabilities conditional on fully observed states. Instead, we simulate the same daily quitting outcomes that we observe in the data and compare the resulting distributions. If we simulate with a discount factor that is too high, simulated drivers will place excessive weight on future wages and will tend to delay exits relative to what is observed. If we simulate with costs that are too low, simulated drivers will quit too rarely during low-wage periods. The discriminator learns which aspects of the observed outcomes reveal such mismatches, and the outer minimization adjusts θ until simulated outcomes match observed outcomes along those dimensions.

4.2. Identification

This subsection provides informal identification intuition for the preference parameters. The goal is to clarify what variation in the data separates forward-looking from myopic behavior and

what variation identifies the distribution of costs, complementing the formal consistency result in Appendix B.1.

Variation in guaranteed wages identifies the cost distribution. Platform A's guaranteed wage w_{it} varies deterministically across shifts and drivers. Holding fixed outside conditions, increases in w_{it} raise the flow payoff from staying on A and reduce quitting. The magnitude and shape of this responsiveness identify (μ_C, σ_C). If costs were nearly homogeneous, quitting would concentrate sharply around a common reservation wage. With heterogeneous costs, quitting responds more smoothly as wages change, reflecting gradual attrition as the net payoff crosses different drivers' cost levels.

Variation in outside options helps identify costs and discounting. Outside opportunities vary over space and time, and we proxy their strength using TLC-based measures of activity on the competing platform, including the shortage index Shortage^B_{lt} constructed in §2.2.1. When Shortage^B_{lt} is high, outside opportunities are locally stronger and exits from A increase. How exits respond to such variation depends on both costs and discounting: high-cost drivers are more prone to exit for a given increase in the outside option, while more myopic drivers place relatively more weight on contemporaneous outside opportunities than on predictable changes in future pay on A.

Variation in continuation values identifies the discount factor. Even when current flow payoffs are similar across platforms, continuation values differ because matching probabilities, trip durations, and future guaranteed wages (on A) vary across time blocks. Because A's wage schedule is pre-announced and changes at known shift boundaries, we observe episodes in which the future value of staying on A changes predictably. Drivers with a higher β adjust behavior in anticipation of these predictable changes, while drivers with a lower β respond primarily to contemporaneous conditions. This intertemporal variation helps pin down how heavily drivers weight future relative to current payoffs.

Preference interpretation. Our preference specification assumes a homogeneous discount factor β common across all drivers and allows heterogeneity only in the per-epoch costs C_i. Within the within-day horizon we study, β should be interpreted as a reduced-form measure of effective planning horizon rather than a separately identified structural time preference parameter. Separately identifying risk attitudes or quasi-hyperbolic discounting would require additional variation that shifts the shape of payoff risk independently of wages and matching conditions; our data do not provide such variation in a clean way.

Under the maintained assumptions that (i) environment primitives are correctly constructed from the proprietary and TLC data (Appendix C.1), (ii) the structural model in §3 is correctly specified, and (iii) drivers' unobserved cost shocks are independent of the constructed outside-option measures conditional on location, time, and day type (Appendix A.1), the adversarial estimator yields consistent estimates of (β, μ_C, σ_C). The third assumption rules out scenarios where unobserved platform A incentives or policies systematically correlate with platform B's local supply-demand conditions. This seems plausible given that the two platforms operated independently during our sample period and neither had real-time visibility into the other's driver availability.

4.3. Target Outcomes and Simulation

We match the joint distribution of when and where drivers quit platform A. These outcomes summarize how drivers respond to time-varying guaranteed wages on A, spatially and temporally varying outside opportunities, and heterogeneity in the local matching environment.

4.3.1. Spatial and temporal discretization. We discretize New York City into $L = 20$ regions: the Bronx, Brooklyn, Newark Liberty International Airport, Central Park, Chelsea, Downtown, Governors Island, Gramercy, Harlem, Lower East Side, Lower West Side, Midtown, Morningside Heights, Upper East Side, Upper West Side, Upper Manhattan, JFK International Airport, LaGuardia Airport, Queens, and Staten Island. We partition each operating day into seven time blocks aligned with platform A's shift structure: 7–9am (AM peak), 9am–12pm (Late AM), 12–2pm (Midday), 2–5pm (Early PM), 5–8pm (PM peak), 8–9pm (PM off peak), and 9pm–midnight (Late night).[4] Within each time block, the model operates on 20-minute decision epochs.

4.3.2. Daily quitting heatmaps. For each day d, location l, and hour h, let $f^d_{l,h}$ denote the fraction of drivers who worked on platform A on day d and exited the platform at location l during hour h. We normalize so that

$$\sum_{l=1}^{L} \sum_{h} f^d_{l,h} = 1 \quad \text{for each day } d.$$

Stacking $\{f^d_{l,h}\}_{l,h}$ into an $H \times L$ matrix yields a daily *quitting heatmap* Q_d. Vectorizing Q_d produces an outcome vector X_d of dimension HL, and stacking $\{X_d\}_d$ across days yields the empirical distribution of spatial-temporal quitting patterns we seek to match.

[4] Our industry partner groups the midday and early PM blocks together into a single midday shift. We break the shift into two blocks to make all blocks more comparable in terms of duration.

4.3.3. Simulation procedure. Given a candidate parameter vector $\theta = (\beta, \mu_C, \sigma_C)$, we simulate driver trajectories and construct simulated outcomes $\{X_d^\theta\}_d$ as follows. For each driver i, we draw a single driver-specific cost C_i from the truncated Normal(μ_C, σ_C) distribution over the support $[\underline{C}, \bar{C}]$. For each driver-day observation in which driver i starts work on platform A, we initialize the driver at the observed start time and location and simulate the within-day sequence of matching events and decisions implied by the model in §3. We simulate match realizations, destinations, and trip durations using the estimated environment primitives, and we draw i.i.d. Type I extreme value shocks to generate the stay/switch/quit choices. We record the simulated quit time and location when the driver exits platform A and aggregate these across drivers to form the simulated heatmap Q_d^θ and vector X_d^θ for day d. §4.4 describes how we evaluate continuation values efficiently during simulation.

4.4. Implementation

Directly solving the dynamic programs for every candidate parameter vector during adversarial estimation would be computationally prohibitive. Each evaluation of the adversarial objective requires simulating a large number of driver trajectories, and each trajectory requires repeated evaluation of continuation values across time and space.

4.4.1. Pre-computation and interpolation. We separate (i) environment primitives that can be estimated once from the data from (ii) preference parameters that must be searched over in estimation. Prior to estimation, we compute matching probabilities, destination distributions, and trip duration distributions for each platform, and we construct the TLC-based measures of outside opportunities described in §2.2.1. We then pre-compute value functions on a grid over (C, β) and store these solutions. During adversarial estimation, we evaluate continuation values for simulated drivers via interpolation over the pre-computed grid rather than re-solving the dynamic programs; Appendix C.1 provides details on the grid design and interpolation scheme.

4.4.2. Discriminator training and parameter updates. We implement the discriminator in (5) as a feed-forward neural network that takes the vectorized daily outcome X_d as input and outputs the probability that the outcome came from the observed data. We train the discriminator using standard stochastic gradient methods and update θ to reduce the discriminator's classification performance. Appendix C.4 provides architectural and training details, and Appendix C.3 provides the derivation of the gradient computations used to update θ.

4.4.3. Inference. We compute standard errors via a bootstrap procedure that resamples days with replacement and re-estimates θ on each bootstrap sample. For each of 100 bootstrap replications, we draw a sample of days with replacement (preserving all driver-day observations within each sampled day), re-estimate environment primitives on the bootstrap sample, and re-run the adversarial estimation procedure. In bootstrap replications where the adversarial optimization does not converge within the iteration limit, we exclude that replication and continue until we obtain 100 successful replications. The reported standard errors are the sample standard deviations of the parameter estimates across successful bootstrap replications.

5. Estimation Results

Table 1 reports the structural estimates from the adversarial indirect inference procedure in Section 4, with bootstrap standard errors (100 replications). We estimate a discount factor of $\hat{\beta} = 0.94985$ per 20-minute decision epoch and substantial heterogeneity in drivers' per-epoch costs of working, with $\hat{\mu}_C = \$0.55358$ and $\hat{\sigma}_C = \$0.66473$ for the truncated Normal specification. Throughout, we interpret β as a reduced-form measure of how drivers trade off current versus future expected earnings within the workday horizon, and we interpret C_i as an incremental cost of remaining active (whether waiting or driving) that can bundle opportunity cost, effort and fatigue, and perceived earnings variability.

5.1. Preference Parameters

Our parameter vector is $\theta = (\beta, \mu_C, \sigma_C)$, where β is the common per-epoch discount factor and (μ_C, σ_C) govern the truncated Normal distribution of per-epoch working costs $C_i \in [\underline{C}, \bar{C}]$.

Table 1 Structural parameter estimates

Parameter	Estimate	95% Confidence Interval
Discount factor per epoch (β)	0.9499	[0.9461, 0.9536]
Mean cost per epoch (μ_C)	\$0.554	[\$0.531, \$0.577]
Std. dev. cost per epoch (σ_C)	\$0.665	[\$0.641, \$0.689]

Note: Estimates rounded to three significant figures. Confidence intervals computed via bootstrap with 100 replications (resampling days with replacement). Each epoch is 20 minutes.

Discount factor and short effective horizons. Gig drivers exhibit substantially shorter planning horizons than documented in traditional employment settings. The estimate $\hat{\beta} = 0.94985$ indicates that drivers place far more weight on near-term earnings than on earnings several hours ahead. Under this exponential discounting, one dollar realized one hour ahead (three epochs) receives weight $0.94985^3 \approx 0.86$; two hours ahead receives weight $0.94985^6 \approx 0.73$; and four hours ahead receives weight $0.94985^{12} \approx 0.54$. For comparison, laboratory studies of intertemporal choice typically find discount factors that imply much longer planning horizons (Frederick et al. 2002), while field studies of labor supply often estimate elasticities consistent with workers smoothing income over weeks or months (Chetty et al. 2011). Our estimates suggest that gig workers operate on markedly shorter horizons, with direct implications for platform design: retention strategies must engage drivers at timescales measured in minutes and hours, not days or weeks.

As discussed in §4.2, our estimated β captures two behavioral factors that both lead drivers to discount future payoffs. The first is standard intertemporal discounting: the rate at which drivers trade off current versus future consumption. The second is responsiveness to uncertainty about future earnings. Even if a driver were patient in a deterministic environment, she would behave as if myopic when future earnings are uncertain and she is risk-averse. Our reduced-form β combines both channels: it measures how drivers actually respond to payoff variations over time given the risky environment they face.

A richer model would separately estimate risk aversion and time preferences, allowing us to distinguish whether drivers discount the future because they are impatient or because they perceive future earnings as risky. However, our data, which captures within-day work decisions but not consumption, wealth, or experimental variation in risk, do not provide sufficient variation to separately identify these parameters. We therefore take the parsimonious approach of letting β absorb both factors. This interpretation aligns with our data, which captures within-day work durations and exit decisions but not consumption, wealth, or direct elicitation of risk preferences. Hereafter, we refer to $\hat{\beta} = 0.94985$ as indicating "substantial myopia" or a "short effective planning horizon" without claiming to have identified deep time preferences.

We highlight that this specification makes our counterfactual estimates conservative: if drivers are, in fact, highly risk-averse, policies that stabilize earnings (such as guaranteed pay) would be even more attractive than our model predicts. Future research with richer data on drivers' outside option uncertainty or experimental variation in earnings risk could decompose these channels and provide sharper predictions.

Cost distribution and heterogeneity. Drivers' perceived costs of working are economically significant but substantially lower than full vehicle operating costs, and exhibit substantial heterogeneity across drivers. The estimated per-epoch cost $\hat{\mu}_C$ = \$0.55 (approximately \$1.66 per hour) is well below full vehicle operating costs reported by industry sources (\$4.40–\$5.48 per hour, Hunter 2014). This suggests that many drivers may not fully internalize their true economic cost of working, consistent with evidence that gig workers often underestimate expenses (Chen et al. 2019).

Drivers exhibit substantial heterogeneity in these costs, with a coefficient of variation near one ($\hat{\sigma}_C/\hat{\mu}_C \approx 1.2$). The estimated model finds that a significant mode of drivers have relatively low perceived costs—these are workers with strong attachment to platform work who remain online even when trip opportunities are limited. However, a substantial tail exhibits high opportunity costs, suggesting a segment of more opportunistic drivers who participate only when conditions are favorable. This heterogeneity helps rationalize the gradual attrition in platform participation we observe as guaranteed wages change over the workday, rather than the sharp exit thresholds that would arise if all drivers had nearly identical costs.

To illustrate heterogeneity beyond the population distribution, we recover a driver-level cost index $\hat{C}_i$ for each driver and plot its empirical distribution in Figure 5.[5] Drivers whose observed sessions persist through low-wage periods tend to have lower posterior costs, while drivers whose sessions end quickly when net pay falls tend to have higher posterior costs.

5.2. Model Fit

The adversarial estimator is designed to match the high-dimensional spatial-temporal pattern of when and where drivers quit platform A. As a summary diagnostic, we compare observed and simulated quitting heatmaps aggregated to the same (time block × region) cells used in estimation. Vectorizing each heatmap and computing the Pearson correlation across cells yields a correlation of 0.75.

This correlation is notably high given the specificity of our model and the inherent stochasticity in real-world outcomes. The model must simultaneously match exit behavior across 20 regions, 7 time blocks per day, and multiple days of the week; a high-dimensional prediction problem where noise is inevitable. Location-specific exit rates vary substantially due to factors we do not model (traffic conditions, customer demographics, driver familiarity with neighborhoods), yet the model

[5] We treat each driver's cost C_i as time-invariant and drawn once per driver, consistent with the model in §3. Conditional on the estimated environment primitives and $\hat{\beta}$, we recover $\hat{C}_i$ using a second-stage procedure described in Appendix A.3. This step is descriptive and does not re-estimate (β, μ_C, σ_C).

Figure 5 Distribution of recovered driver-level cost indices

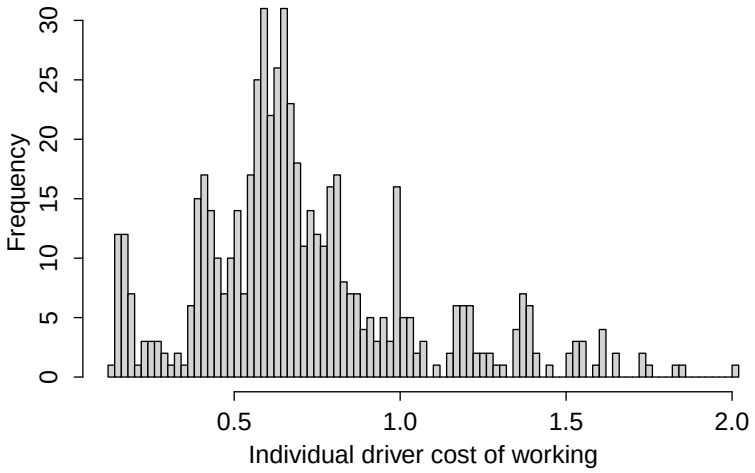

Note: Each driver's cost index $\hat{C}_i$ is the posterior mean of C_i under the estimated truncated Normal prior and a simulated likelihood based on the driver's observed session start and termination outcomes; see Appendix A.3.

captures three-quarters of this variation. For this context, where drivers face stochastic matching and make frequent decisions under uncertainty, a correlation of 0.75 indicates that the estimated primitives successfully reproduce the main structure of observed behavior. Additional fit diagnostics are provided in Appendix A.4.

Wage elasticity and switching behavior. Drivers exhibit high wage elasticity, rapidly reallocating across platforms in response to pay changes. Figure 7 provides striking evidence of this price responsiveness: switching propensity, the probability that an active driver exits platform A for the competing platform, spikes sharply at shift boundaries when guaranteed wages change. The three prominent spikes occur at 9am (when the high morning wage ends), 5pm (when the afternoon peak wage begins), and 8pm (when the peak wage ends). Between these boundaries, switching rates remain low and stable, indicating that drivers who commit to platform A at the prevailing wage tend to complete their intended work session.

This pattern directly demonstrates wage elasticity in platform choice. When platform A changes its guaranteed wage at a shift boundary, we observe significant immediate changes in labor supply as drivers compare the new wage to outside options and switch platforms if the competing platform becomes more attractive. The combination of short planning horizons and cost heterogeneity amplifies this elasticity: drivers decide whether to stay or to switch by comparing current-period payoffs rather than averaging over longer horizons, making them highly responsive to discrete wage changes.

Figure 6 reinforces this finding from a different angle. Utilization rates, the fraction of drivers remaining active on platform A, respond systematically to the guaranteed wage schedule. Utilization peaks during midday and afternoon rush hours when wages are highest, then declines sharply at shift boundaries when wages fall. This pattern reflects both the estimated cost heterogeneity (high-cost drivers exit first when wages drop) and the short planning horizons (drivers respond immediately to wage changes rather than smoothing work decisions over longer periods).

Taken together, these patterns reveal that platform labor supply is highly wage elastic at short time horizons. Platforms competing for multihoming workers face drivers who continuously compare pay conditions and reallocate quickly when relative compensation shifts. This has direct implications for platform strategy: small wage changes can generate large supply responses within hours, making wage competition particularly intense in markets with multihoming workers.

Figure 6 Simulated utilization rates by time of day

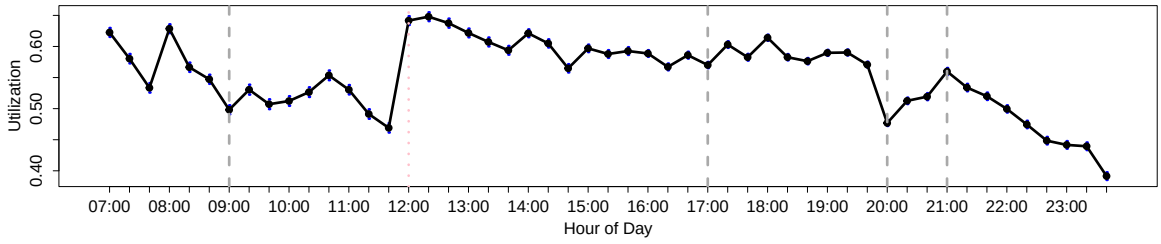

Note: Grey dashed lines represent shift boundaries; the dotted line marks noon. Patterns generated using estimated parameters $(\hat{\beta}, \hat{\mu}_C, \hat{\sigma}_C)$.

Figure 7 Simulated switching probabilities by time of day

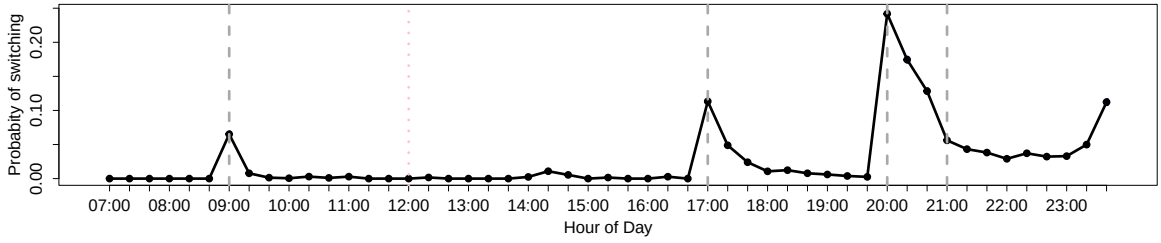

Note: Grey dashed lines represent shift boundaries; the dotted line marks noon. Patterns generated using estimated parameters $(\hat{\beta}, \hat{\mu}_C, \hat{\sigma}_C)$. Switching spikes at shift boundaries reflect drivers' high wage elasticity.

Finally, we emphasize what the model is, and is not, designed to fit. We condition on drivers who have already started the workday on platform A and focus on within-day stay, switch, and quit

incentives. We do not target the extensive margin of whether to work at all on a given day, and we do not calibrate to summary outcomes such as total daily trip counts that may be driven by factors outside the within-day incentives captured by the model.

5.3. Model-Implied Multihoming Patterns

Single-platform data do not directly observe whether and when a driver works on the competing platform during a day. The estimated model, however, implies a within-day switching process, so we can summarize multihoming behavior under the estimated parameters. We simulate driver trajectories using $(\hat{\beta}, \hat{\mu}_C, \hat{\sigma}_C)$ and compute the fraction of workdays in which a driver switches from platform A to platform B.

Under the estimated model, 66.59% of platform A drivers multihome during the majority of days they work. Among all drivers, 42.23% multihome every day they work, while 16.01% never multihome. These magnitudes highlight that, in the model, switching is a quantitatively important margin for understanding platform A's ability to retain active supply over the day.

The timing of switching in Figure 7 further shows that multihoming incentives vary systematically within the day. In the model, switching propensity increases when the guaranteed wage on A changes and when the outside option on B becomes locally attractive. The next section uses these estimated primitives to evaluate counterfactual compensation policies and to quantify how changes in the guaranteed pay schedule affect retention and multihoming.

6. Counterfactual Analyses

Our structural estimates reveal strong myopia among gig drivers. This creates a fundamental challenge for platforms: pay design must engage workers at horizons measured in minutes and hours, not days or weeks. A platform offering high expected daily earnings but variable hourly pay may lose capacity to a competitor offering lower but more predictable compensation. Similarly, policies aimed at raising worker welfare must account for how quickly workers reallocate in response to changes in posted wages.

We use the estimated model to address three questions. First, can guaranteed hourly pay retain capacity when competing against attractive pay-per-work schemes (§6.1)? Guaranteed pay provides stable compensation within each hour, which aligns with short-horizon behavior, but requires paying even when trips are scarce. Pay-per-work mirrors real-time demand but shifts idle-time risk to workers. Second, how do short-term retention levers like streak bonuses and quit delays perform when layered on guaranteed pay (§6.2)? Both extend sessions, but do they reduce or increase

multihoming? Third, we validate the model by comparing its predictions to observed outcomes from NYC's 2019 minimum-wage policy (§6.3). The rule raised posted per-trip rates but generated congestion; we test whether the model correctly predicts the resulting changes in both earnings and idle time.

Together, these counterfactuals demonstrate that managing myopic supply is tractable but requires aligning pay timing with workers' decision horizons. Platforms can retain capacity through predictable compensation and carefully designed short-term incentives. Policymakers can raise effective wages, but only if wage floors are paired with tools to manage the congestion they create.[6]

6.1. Guaranteed Pay versus Pay-Per-Work

Gig platforms must keep enough workers online to meet fluctuating demand. Two pay designs dominate in practice. *Pay-per-work* compensates drivers only for completed trips. Earnings track real-time supply and demand: high when trips are abundant, zero while waiting. *Guaranteed hourly pay* compensates drivers for time online and available, regardless of trip volume. Our focal platform uses guaranteed pay, as do GoPuff, Postmates, and DoorDash for workers who opt in (Browning 2023).

The operational question is whether guaranteed pay can compete with attractive pay-per-work when workers focus on near-term earnings. Pay-per-work offers high pay during busy periods and clears imbalances by letting drivers leave when work is scarce. Guaranteed pay provides stable compensation, which evidence suggests can extend work duration (DeVoe and Pfeffer 2007), but requires paying even during thin periods. Which design better retains capacity when workers are myopic and multihome?

Design. We compare the two schemes on four outcomes: hours online on the focal platform, trips completed, switching rates to the competitor, and daily earnings. We hold demand, matching rates, and trip characteristics fixed so differences arise purely from the pay rule.

Direct comparison requires putting the two schemes on common ground. Guaranteed pay compensates time online; pay-per-work compensates only completed trips. We construct a benchmark per-trip schedule that delivers the same expected hourly earnings as the observed guaranteed schedule. For driver i in hour t, we set per-trip rate r_{it} such that

$$w_{it} = r_{it} \cdot R_t \cdot \frac{60}{\tau_t},$$

[6] In all counterfactuals, we maintain the one-way switching structure from the estimated model. After a driver switches from the focal platform to the competitor, she does not switch back the same day. This matches observed patterns and keeps the state space tractable. It makes our retention estimates conservative: in markets where some drivers return after sampling competitors, platforms would not need to offer as much compensation to preserve capacity.

where w_{it} is the guaranteed hourly rate, R_t is matching probability, and τ_t is average trip duration in minutes. This 1× benchmark preserves time-of-day patterns while making the comparison economically meaningful. We then examine per-trip rates from 0.5× to 4× the benchmark to determine how much pay-per-work compensation is needed to match guaranteed pay's capacity and retention.

Results: Hours and trips. At the 1× benchmark where expected earnings are equalized, pay-per-work produces fewer hours and trips than guaranteed pay (Figure 8). To match guaranteed-pay capacity, per-trip rates must rise to 1.25×–1.5×. The required premium varies by weekday but the pattern holds: drivers work longer under guaranteed pay when expected earnings are equalized.

Figure 8 Daily hours and trips by weekday: guaranteed pay versus pay-per-work

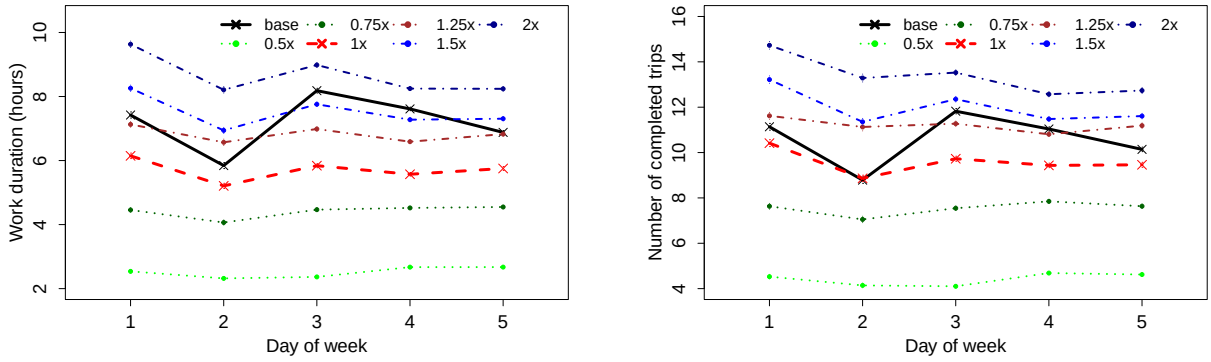

(a) Daily hours online

(b) Trips completed

Note: "Base" is guaranteed pay. "·×" denotes per-trip rate as multiple of equivalent benchmark. Weekdays: 1=Monday,...,5=Friday.

Results: Retention. Pay design shapes platform loyalty; however, loyal drivers require substantially higher per-trip pay to remain loyal under pay-per-work. We classify drivers by switching frequency: *never-switchers* (never switch to competitor), *mostly-switchers* (switch ≥50% of days), and *always-switchers* (switch every day). To retain the same share of never-switchers as under guaranteed pay, per-trip rates must reach 2.5×–3× (Figure 9a). For mostly-switchers, 1.5×–2× is needed (Figure 9b). For always-switchers, 1×–1.25× suffices (Figure 9c).

Results: Earnings. At 1×, pay-per-work yields 30% higher hourly earnings than guaranteed pay (Figure 10a) because work concentrates in high-demand periods. However, daily earnings are similar (Figure 10b): drivers earn more per hour but work fewer hours. From the platform's perspective, guaranteed pay achieves similar daily earnings while keeping drivers online longer, providing more capacity to absorb demand fluctuations.

Figure 9 Multihoming by driver type: guaranteed pay versus pay-per-work

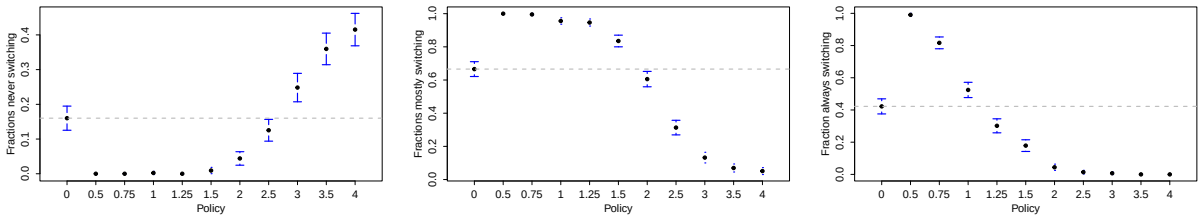

(a) Never-switchers (b) Mostly-switchers (c) Always-switchers

Note: Grey dashed lines mark baseline shares. See Appendix D.1.2 for weekday-level patterns.

Figure 10 Driver earnings: guaranteed pay versus pay-per-work

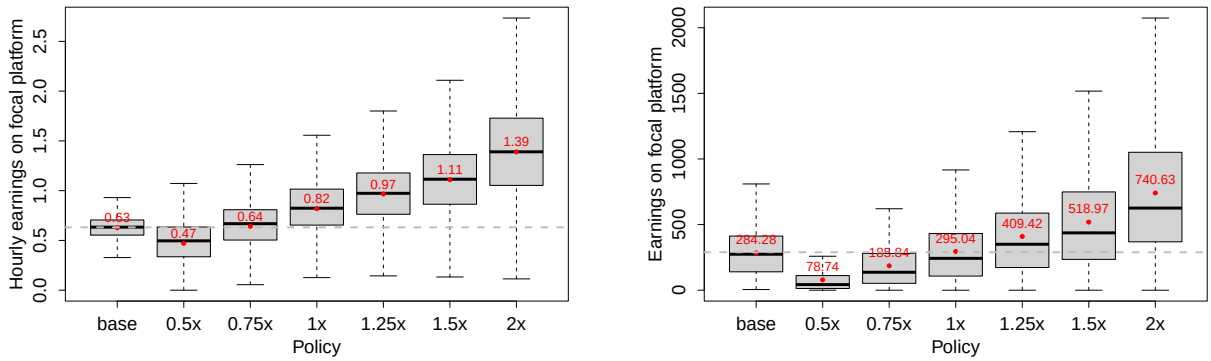

(a) Hourly earnings (b) Daily earnings

Note: Grey dashed lines mark guaranteed-pay baseline. See Appendix D.1.1 for full outcome distributions.

Interpretation. Our estimates suggest that guaranteed hourly pay offers a cost-effective approach to building capacity when workers decide over short horizons. At equal expected earnings, i.e., a fixed labor cost to the firm, drivers stay longer and switch less under guaranteed pay. The differences arise from timing and predictability, not average pay levels. Our comparison holds demand and matching fixed; the benchmark per-trip schedule matches guaranteed pay in expected hourly earnings. The results isolate how short-horizon drivers respond to predictable versus variable earnings streams.

Pay-per-work must offer substantially higher rates, especially for loyal drivers, to match guaranteed pay's retention. This aligns with evidence that workers value stable earnings (DeVoe and Pfeffer 2007). Many drivers accept lower peak hourly earnings for predictability, and platforms benefit through lower labor costs for maintaining steady capacity. Our estimates assume one-way switching within days. If some drivers return after sampling competitors, the per-trip premium for preserving loyalty would be lower. Our estimates are therefore conservative from the focal platform's perspective.

6.2. Streak Bonuses vs. Quit Delays

Beyond long-run pay design, platforms use short-term levers operating at the scale of an hour or less. We study two common tools: streak bonuses and quit delays.

Streak bonuses reward sustained activity. Lyft's "Ride Streak" pays drivers completing consecutive trips within a time window. DoorDash offers "Guaranteed Earnings" for completing set deliveries within a week. These bonuses raise the marginal benefit of the next job on the current platform. Evidence shows threshold incentives can be effective, especially for engaged workers (Kabra et al. 2017, Liu et al. 2023), and concrete goals motivate effort (Locke 1996).

Quit delays change exit timing. When a driver signals she wants to stop, the platform keeps her online for a short period and may assign one last trip. Uber has experimented with such nudges (Scheiber 2017). Many platforms pre-assign the next trip before the current ends, locking drivers in. This has little direct cost since base pay continues, but introduces friction. It can discourage chasing outside options immediately, yet may prompt drivers to switch earlier to avoid being locked in during low-demand periods (Tadepalli and Gupta 2020).

Which lever better extends sessions and preserves loyalty when layered on guaranteed pay?

Design. We compare three policies: baseline guaranteed pay, a time-delay policy (drivers wait one 20-minute epoch before logging off), and a consecutive-work bonus policy (drivers earn an additional bonus for staying active a full clock hour). We hold demand and guaranteed wages fixed. We measure daily hours on the focal platform and multihoming rates.

Results. Both policies extend hours relative to baseline. Drivers with bonuses work slightly longer than those facing delays (Figure 11a). However, effects on multihoming differ sharply. Baseline multihoming is 67%. Time delays raise this to over 80%. Consecutive-work bonuses reduce it substantially (Figure 11b). Utilization and daily earnings change little under either policy; the main effects are session length and switching frequency.

Interpretation. The contrast is informative. Consecutive-work bonuses make staying to complete the hour attractive, reducing switching. Drivers who commit to several epochs value collecting the bonus. Time delays work differently. Because delays trigger when drivers attempt to quit, effects depend on current conditions. When utilization is low, delays force waiting in unattractive states. Anticipating this, drivers switch earlier to avoid being locked in later. This shows up as higher multihoming despite longer hours.

For guaranteed-pay platforms, this state dependence can be useful. Paying guarantees to underutilized drivers is costly. Time delays nudge excess supply toward competitors while occasionally

Figure 11 Hours and multihoming: bonuses versus delays

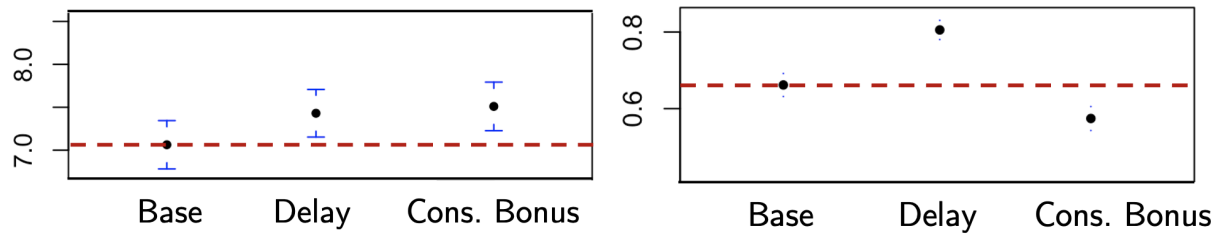

(a) Daily hours on focal platform (b) Multihoming rates

Note: "Base" is guaranteed pay. "Delay" requires 20-minute wait before quitting. "Cons. Bonus" rewards staying active one full hour. Red dashed lines mark baseline.

capturing trips during delays. But delays don't build loyalty. Consecutive-work bonuses and quit delays are not interchangeable. Bonuses are blunt but effective for retention. Delays extend hours but encourage strategic multihoming. Even when workers are insulated from earnings risk, short-horizon incentive design shapes where they work.

6.3. Model Validation: NYC Minimum-Wage Policy

We use NYC's 2019 minimum-wage policy as a partial validation of the model's predictions. In December 2018, the Taxi and Limousine Commission adopted *Driver Income Rules* requiring ride-hailing drivers earn at least $17.22 per hour of work, with pay reflecting time and distance.[7] The rule was motivated by analysis from Parrott and Reich (2018) documenting low effective earnings among NYC drivers. Enforcement began in early 2019 for major platforms paying per trip. Our industry partner (platform A), which pays guaranteed hourly wages, was exempt.

Our data cover summer 2017, before implementation. We simulate how drivers starting on platform A respond when the competing platform B raises wages to meet the minimum.[8] This setting differs from the empirical evaluations, which measure market-wide effects when all major platforms were subject to the rule. Nevertheless, comparing model predictions to observed outcomes provides a check on whether estimated driver myopia correctly predicts responses to wage changes in matching markets.

Design. We simulate two scenarios: (1) pre-2019 baseline matching our estimation sample, and (2) actual 2019 implementation where the rule applies to platform B but not platform A. We hold

[7] https://nyc.gov/assets/tlc/downloads/pdf/driver_income_rules_12_04_2018.pdf

[8] This validation has important limitations: our model uses 2017 data to predict responses to a 2019 policy, and our partial-enforcement scenario (one exempt platform) differs from the actual universal enforcement. We interpret this as testing whether the model captures the *mechanism* (myopic supply response → congestion) rather than precise magnitudes. See Appendix D.2 for detailed discussion of these limitations and comparison with empirical studies.

demand and fares fixed, consistent with evidence that platforms adjusted primarily through driver access rather than large fare increases (Koustas et al. 2020).

The rule raises minimum per-trip compensation on B to ensure drivers earn ≥$17.22 per hour of work. We adjust per-trip rate r_{lt} so expected hourly earnings meet the minimum, mirroring how platforms adjusted pay structures in practice. We focus on how the policy affects drivers who start their day on platform A: do they switch more to B when B's wages rise? Do their total daily earnings change?

Model predictions. Table 2 reports the model's predictions. When platform B raises wages to meet the minimum, drivers starting on A experience a 3.5% decline in daily earnings and a 2.1% increase in idle time. The earnings decline occurs because more drivers enter platform B or switch from A to B earlier in their shifts, attracted by higher posted rates. With demand held fixed, the additional supply on B creates congestion. Drivers spend more time waiting between trips, which offsets the higher per-trip rates. Even though hourly rates on B rise, effective earnings fall because drivers work fewer productive hours.

Table 2 Model predictions and empirical evidence on minimum-wage effects

	Model prediction (Platform B only)	Empirical evidence (All platforms)
Immediate effects:		
Idle time or hours worked	+2.1% idle time	−8% to −12% hours
Net earnings effect:		
Daily/weekly/monthly earnings	−3.5%	−5.4% to −1.2%[a]

Notes: Model predictions are for drivers starting on platform A (exempt) when platform B (competitor) implements minimum wage. Empirical evidence from Koustas et al. (2020) for NYC (all platforms subject) and An et al. (2025) for Seattle delivery workers (all platforms subject). Direct comparison is limited because empirical studies measure market-wide enforcement while our model examines partial enforcement with one exempt platform.

[a]Koustas et al. (2020) reports −5.4% for NYC weekly earnings [95% CI: −10.2%, −0.6%]; An et al. (2025) report −1.2% for Seattle monthly earnings [95% CI: −9.6%, 7.2%, not significant].

Comparison to empirical patterns. Empirical work on wage floors in matching markets often finds that posted pay increases, but realized earnings can remain flat or decline once labor supply adjusts and/or platforms ration access. For example, Koustas et al. (2020) evaluate NYC's policy

using difference-in-differences, comparing NYC drivers (treated) to New Jersey drivers (control) after February 2019. He finds hourly pay rose 7.5% but weekly earnings fell 5.4% [95% CI: −10.2%, −0.6%], driven by a 12% decline in hours worked. An et al. (2025) study Seattle's parallel policy for delivery workers and find base pay per task rose 34% but monthly earnings remained flat at −1.2% [95% CI: −9.6%, 7.2%, not significant], driven by an 8.2% decline in orders per worker. While the institutional settings and enforcement scope differ from our counterfactual, the model generates the same qualitative tension: raising posted pay can attract supply or induce switching, which can increase waiting or reduce productive time when demand is held fixed.

Mechanism within the model. In our simulations, the wage floor raises the attractiveness of platform B in the near term. Given the estimated short-horizon tradeoff embedded in $\hat{\beta}$, drivers respond by reallocating more quickly toward B. Holding demand fixed, this reallocation increases congestion on B in the sense of more time spent between matches. The resulting increase in idle time offsets part of the mechanical increase in posted pay, leading to lower realized earnings for drivers who switch.

This mechanism is distinct from platform-side access restrictions. In the model, drivers can remain online but experience more waiting; in practice, platforms may also respond by limiting access or otherwise reducing active supply during low-demand periods (Koustas et al. 2020). Both channels operate in the same direction in that they can reduce realized earnings gains even when posted compensation rises.

Policy implications. The consistency between model predictions and empirical evidence, despite differences in scope, suggests the estimated preference parameters correctly capture how gig workers respond to wage changes. The policy lesson is that minimum-wage rules in matching markets generate congestion effects that can offset nominal wage gains. Koustas et al. (2020) show platforms responded through rationing; An et al. (2025) show customers responded through lower tips. Our model highlights a third margin: drivers' own myopic reallocation decisions create congestion even before platforms adjust access policies.

For policymakers, this suggests minimum-wage rules are most effective when paired with tools to manage congestion: caps on active drivers, priority scheduling during peak demand, or dynamic pricing that maintains market balance. Without such tools, wage floors can redistribute hours or idle time without raising total worker welfare. The interaction between wage floors and pay schemes also matters. Appendix D.3 explores hypothetical scenarios with enforcement on guaranteed-pay platforms or universally, showing that broader enforcement amplifies congestion without proportionally raising earnings.

This partial validation exercise demonstrates that the model captures key behavioral responses to policy changes, even in an out-of-sample setting with a fundamentally different market structure than our estimation sample. The model provides a credible tool for evaluating other interventions in gig labor markets where workers make decisions over short horizons.

7. Concluding Remarks

This paper studies how gig platforms should manage labor supply when workers multihome across competing platforms within the workday. The operational challenge is to retain capacity when workers can reallocate quickly in response to time-varying pay and outside opportunities.

Our analysis contributes on three dimensions. First, we address a pervasive feature of industry data: event-driven logging. In our setting, the platform records rich state information at session start and termination but not at intermediate epochs when a driver chooses to continue. Because observability depends on (choice) outcomes, standard dynamic discrete choice estimation based on fully observed per-epoch states is not directly applicable, and conditioning on selectively observed states can raise selection concerns. We show that adversarial estimation provides a practical alternative by recovering preference parameters through matching consistently observed, high-dimensional aggregate outcomes. In particular, we implement an estimator that matches spatial-temporal quitting patterns by combining structural simulation with a discriminator network.

Second, we provide evidence on worker decision-making in competitive gig markets. Applied to NYC ride-hailing, the estimated preference parameters imply short planning horizons over within-day decisions and substantial heterogeneity in drivers' perceived costs of remaining active. These features jointly rationalize frequent within-day reallocation across platforms.

Third, we use the estimated model to inform pay design and regulation under multihoming. In counterfactuals that hold demand and the matching environment fixed, guaranteed hourly pay retains more capacity than pay-per-work at comparable expected earnings because predictable compensation aligns with short decision horizons. Short-term levers also have distinct effects: streak-style bonuses that reward consecutive work can reduce multihoming, whereas operational frictions that delay exit may backfire by inducing earlier switching in anticipation of being locked in during unattractive future states. A policy exercise based on NYC's Driver Income Rules yields predictions consistent with the empirical pattern that higher posted pay can attract supply and increase congestion, muting realized earnings gains, which highlights the importance of pairing wage floors with congestion-management tools.

Several limitations point to extensions. We abstract from platform-side responses such as access rationing, and incorporating equilibrium adjustments would clarify when guaranteed pay remains viable as both sides optimize. We model within-day switching as absorbing, consistent with observed behavior but potentially conservative in markets where workers sample competitors and return. We assume homogeneous discounting, and separating time preferences from risk aversion would require richer variation in payoff distributions. Finally, we focus on two platforms; extending to settings with multiple platforms would clarify competitive dynamics under multihoming.

We close with two broader takeaways. Methodologically, adversarial estimation is a useful addition to the structural toolkit when key states are only observed at events, not at every decision epoch. Substantively, the results emphasize that platforms compete at the timescale at which workers decide. When planning horizons are measured in minutes and hours, retention depends less on average earnings and more on the timing, predictability, and short-horizon incentives embedded in pay. Designing those incentives well can make multihoming supply manageable rather than destabilizing.

References

Allon G, Chen D, Moon K (2025) Measuring strategic behavior by gig economy workers: Multihoming and repositioning. *Available at SSRN 4411974* .

Allon G, Cohen MC, Sinchaisri WP (2023) The impact of behavioral and economic drivers on gig economy workers. *Manufacturing & Service Operations Management* 25(4):1376–1393.

An Y, Garin A, Kovak B (2025) Delivering higher pay? the impacts of a task-level pay standard in the gig economy .

Andersen S, Di Girolamo A, Harrison GW, Lau MI (2014) Risk and time preferences of entrepreneurs: evidence from a danish field experiment. *Theory and decision* 77(3):341–357.

Anderson M, McClain C, Faverio M, Gelles-Watnick R (2021) The state of gig work in 2021 .

Athey S, Calvano E, Gans JS (2018) The impact of consumer multi-homing on advertising markets and media competition. *Management cience* 64(4):1574–1590.

Athey S, Castillo JC, Chandar B (2024) Service quality on online platforms: Empirical evidence about driving quality at uber. Technical report, National Bureau of Economic Research.

Benjaafar S, Ding JY, Kong G, Taylor T (2022) Labor welfare in on-demand service platforms. *Manufacturing & Service Operations Management* 24(1):110–124.

Benjaafar S, Hu M (2020) Operations management in the age of the sharing economy: what is old and what is new? *Manufacturing & Service Operations Management* 22(1):93–101.

Benjaafar S, Xiao S, Yang X (2020) Do workers and customers benefit from competition between on-demand service platforms? *Available at SSRN 3645882* .

Bernstein F, DeCroix GA, Keskin NB (2021) Competition between two-sided platforms under demand and supply congestion effects. *Manufacturing & Service Operations Management* 23(5):1043–1061.

Besbes O, Castro F, Lobel I (2021) Surge pricing and its spatial supply response. *Management Science* 67(3):1350–1367.

Besbes O, Goyal V, Iyengar G, Singal R (2022) Effective wages under workforce scheduling with heterogeneous time preferences. *Available at SSRN* .

Bolton GE, Katok E, Ockenfels A (2004) How effective are electronic reputation mechanisms? an experimental investigation. *Management science* 50(11):1587–1602.

Browning K (2023) Doordash, shifting business model, will offer drivers hourly pay. URL https://www.nytimes.com/2023/06/28/business/doordash-hourly-wage-option.html.

Bryan KA, Gans JS (2019) A theory of multihoming in rideshare competition. *Journal of Economics & Management Strategy* 28(1):89–96.

Butschek S, Amor RG, Kampkötter P, Sliwka D (2022) Motivating gig workers–evidence from a field experiment. *Labour Economics* 75:102105.

Cameron L, Meuris J (2022) The peril of paycheck dispersion: When fluctuations in compensation jeopardize worker retention. *Academy of Management Proceedings*, volume 2022, 15162 (Academy of Management Briarcliff Manor, NY 10510).

Cattaneo MD, Ma X, Masatlioglu Y, Suleymanov E (2020) A random attention model. *Journal of Political Economy* 128(7):2796–2836.

Cennamo C, Ozalp H, Kretschmer T (2018) Platform architecture and quality trade-offs of multihoming complements. *Information Systems Research* 29(2):461–478.

Chen L, Cui Y, Liu J, Liu X (2022) Bonus competition in the gig economy. *Available at SSRN 3392700* .

Chen MK, Rossi PE, Chevalier JA, Oehlsen E (2019) The value of flexible work: Evidence from uber drivers. *Journal of Political Economy* 127(6):2735–2794.

Chetty R, Friedman JN, Olsen T, Pistaferri L (2011) Adjustment costs, firm responses, and micro vs. macro labor supply elasticities: Evidence from danish tax records. *The quarterly journal of economics* 126(2):749–804.

Chitla S, Cohen M, Jagabathula S, Mitrofanov D (2023) Customers' multihoming behavior in ride-hailing: Empirical evidence using a structural model. *Working Paper* .

Choudhary V, Shunko M, Netessine S, Koo S (2022) Nudging drivers to safety: Evidence from a field experiment. *Management Science* 68(6):4196–4214.

Critero (2017) URL https://www.criteo.com/wp-content/uploads/2017/10/TheShopperStory_US_Final.pdf.

Davies J, Khodjamirian S, Giallombardo F, Aletti P (2022) Survey evidence on multi-homing in online retail business. URL https://www.compasslexecon.com/the-analysis/survey-evidence-on-multi-homing-in-online-retail-businesses/11-23-2022/.

DeVoe SE, Pfeffer J (2007) When time is money: The effect of hourly payment on the evaluation of time. *Organizational Behavior and Human Decision Processes* 104(1):1–13.

Dong J, Ibrahim R (2020) Managing supply in the on-demand economy: Flexible workers, full-time employees, or both? *Operations Research* .

Fitzsimmons EG (2018) Uber hit with cap as new york city takes lead in crackdown. URL https://www.nytimes.com/2018/08/08/nyregion/uber-vote-city-council-cap.html.

Frederick S, Loewenstein G, O'donoghue T (2002) Time discounting and time preference: A critical review. *Journal of economic literature* 40(2):351–401.

Goeree MS (2008) Limited information and advertising in the us personal computer industry. *Econometrica* 76(5):1017–1074.

Goodfellow I, Pouget-Abadie J, Mirza M, Xu B, Warde-Farley D, Ozair S, Courville A, Bengio Y (2014) Generative adversarial nets. *Advances in neural information processing systems* 27.

Gourieroux C, Monfort A, Renault E (1993) Indirect inference. *J. Appl. Econometrics* 8(S1):S85–S118.

Hunter H (2014) Owning and operating your vehicle just got a little cheaper according to aaa's 2014 'your driving costs' study. *AAA NewsRoom* .

Ibrahim R (2018) Managing queueing systems where capacity is random and customers are impatient. *Production and Operations Management* 27(2):234–250.

Ikeda K, Bernstein MS (2016) Pay it backward: Per-task payments on crowdsourcing platforms reduce productivity. *Proceedings of the 2016 CHI Conference on Human Factors in Computing Systems*, 4111–4121.

Kabra A, Elena B, Karan G (2017) The efficacy of incentives in scaling marketplaces, working paper.

Kaji T, Manresa E, Pouliot G (2023) An adversarial approach to structural estimation. *Econometrica* 91(6):2041–2063.

Koustas D, Parrott JA, Reich M (2020) New york city's gig driver pay standard: Effects on drivers, passengers, and the companies .

Laibson D (1997) Golden eggs and hyperbolic discounting. *The Quarterly Journal of Economics* 112(2):443–478.

Landsman V, Stremersch S (2011) Multihoming in two-sided markets: An empirical inquiry in the video game console industry. *Journal of Marketing* 75(6):39–54.

Li H, Zhu F (2021) Information transparency, multihoming, and platform competition: A natural experiment in the daily deals market. *Management Science* 67(7):4384–4407.

Liu T, Xu Z, Vignon D, Yin Y, Li Q, Qin Z (2023) Effects of threshold-based incentives on drivers' labor supply behavior. *Transportation Research Part C: Emerging Technologies* 152:104140.

Lobel I, Martin S, Song H (2024) Frontiers in operations: Employees vs. contractors: An operational perspective. *Manufacturing & Service Operations Management* 26(4):1306–1322.

Locke EA (1996) Motivation through conscious goal setting. *Applied and preventive psychology* 5(2):117–124.

Loginova O, Wang XH, Liu Q (2022) The impact of multi-homing in a ride-sharing market. *The Annals of Regional Science* 69(1):239–254.

Mai Y, Hu B, Pekeč S (2023) Courteous or crude? managing user conduct to improve on-demand service platform performance. *Management Science* 69(2):996–1016.

Mas A, Pallais A (2017) Valuing alternative work arrangements. *American Economic Review* 107(12):3722–3759.

Miao W, Deng Y, Wang W, Liu Y, Tang CS (2022) The effects of surge pricing on driver behavior in the ride-sharing market: Evidence from a quasi-experiment. *Journal of Operations Management* .

Moon K (2023) Strategic path selection in service networks: Leveraging machine learning to estimate combinatorially complex preferences for consumption and waiting. *Available at SSRN 3819117* .

O'donoghue T, Rabin M (1999) Doing it now or later. *American economic review* 89(1):103–124.

Pakes A, Pollard D (1989) Simulation and the asymptotics of optimization estimators. *Econometrica: Journal of the Econometric Society* 1027–1057.

Park KF, Seamans R, Zhu F (2021) Homing and platform responses to entry: Historical evidence from the us newspaper industry. *Strategic Management Journal* 42(4):684–709.

Parrott JA, Reich M (2018) An earnings standard for new york city's app-based drivers. *New York: The New School: Center for New York City Affairs* .

Rosaia N (2025) Competing platforms and transport equilibrium. *Econometrica* 93(6):2235–2271.

Scheiber N (2017) How uber uses psychological tricks to push its drivers' buttons. *Ethics of Data and Analytics*, 362–371 (Auerbach Publications).

Shokoohyar S, Katok E (2022) Incentivizing suppliers using scorecard: A behavioral study. *Journal of the Operational Research Society* 73(5):1105–1126.

Tadepalli K, Gupta A (2020) Multihoming in ridesharing markets: Welfare and investment. *Working Paper* .

Wilson R (2019) Seattle becomes first city to cap uber, lyft vehicles. URL https://www.washingtonpost.com/blogs/govbeat/wp/2014/03/18/seattle-becomes-first-city-to-cap-uber-lyft-vehicles/.

E-Companion to "*Managing Multihoming Workers in the Gig Economy*"

Appendix A: Additional Details on Data and Environment

A.1. Construction of Outside Option Measures

Our structural model represents the outside option by a single competing ride-hailing platform, denoted B. We construct platform B's time- and location-specific attractiveness using public TLC trip records and posted fare schedules. This appendix explains how this simplification relates to the broader market and to other types of gig work.

Other ride-hailing platforms. During our study period (July 2017), New York City's ride-hailing market included several platforms beyond our partner firm. Trip volumes were highly concentrated among a small number of large firms. The TLC trip records show that the bulk of car-based ride-hailing activity is accounted for by our focal partner and one dominant competitor. We refer to the largest competitor as platform B throughout. Remaining platforms have much smaller trip volumes.

We interpret platform B as a representative outside ride-hailing platform. More precisely, the outside option in our model represents a composite of all technologically similar opportunities: driving for B, driving for smaller car-based ride-hailing platforms, or taking another car-based job with comparable effort and schedule flexibility. We use B as the basis for our outside-option proxy because we observe its trip volumes and implied fare-based earnings at the neighborhood-by-time level from TLC records. This provides disciplined variation in outside conditions that we can align with drivers' exit behavior from A. Smaller platforms do not offer similarly detailed public data.

Our identification strategy does not require observing where each driver goes after leaving A. We observe the full sequence of locations and times at which drivers are active on A. We observe, from TLC records, the neighborhood-by-time imbalance between dropoffs and pickups and the implied surge-like conditions on B. We use temporal and spatial variation in B's attractiveness to discipline the switching margin: when the shortage proxy for B spikes in a specific neighborhood and hour, we see a corresponding increase in exits from A at that neighborhood and hour. The model interprets such exits as switching to attractive outside options. When exits occur late in the day or when B's shortage index is low, the model attributes more of that behavior to quitting for the day. Identification comes from variation in market tightness on B, not from assuming that every exit is a switch to B.

Non-ride-hailing outside options. Drivers on A may have access to gig opportunities outside of car-based ride-hailing, such as app-based restaurant delivery. We do not model these alternatives explicitly because the dominant mode of app-based restaurant delivery in New York City is non-car based. A 2022 study by the New York City Department of Consumer and Worker Protection reports that more than 80% of app-based restaurant delivery workers rely primarily on e-bikes (New York City Department of Consumer and Worker Protection 2022). Although this evidence covers 2021-2022, several years after our 2017 study period, it documents the mature modal mix once that sector fully developed. The predominance of e-bikes is consistent with long-standing delivery patterns in the city and suggests that app-based restaurant delivery attracts a worker pool technologically distinct from the car-based drivers in our sample.

From the perspective of our structural model, any non-ride-hailing option available to a driver at exit from A raises the outside option value relative to the benchmark we construct from B's conditions. If a driver exits A when B's shortage proxy is low but takes an unmodeled job offering a higher payoff, the true outside value exceeds our proxy. This

makes our outside-option measure conservative rather than overstated. It does not overturn the qualitative mechanisms we identify, which depend on the relative volatility and predictability of pay on A versus the outside option, not on the precise composition of the outside option.

A.2. Interpretation of Estimated Cost Parameters

The estimated mean per-epoch cost $\hat{\mu}_C = \$0.55358$ (approximately \$1.66 per hour) requires careful interpretation. This magnitude is substantially below industry estimates of full vehicle ownership and operating costs. The 2014 American Automobile Association report (Hunter 2014) estimates total vehicle operating costs that imply roughly \$4.40–\$5.48 per hour under our speed conversion assumptions for NYC traffic conditions.

The gap between our estimate and these benchmarks reflects the reduced-form nature of our cost parameter. Specifically, C_i serves as a sufficient statistic for drivers' quit decisions and bundles several conceptually distinct factors:

1. **Marginal vehicle operating costs:** Fuel consumption and vehicle wear that vary with driving intensity, but excluding fixed costs like insurance and depreciation that are incurred regardless of work decisions.
2. **Opportunity cost of time:** The value of alternative uses of time, including other gig work, household production, or leisure.
3. **Effort and fatigue:** Physical and mental costs of remaining active, including driving, navigating, and interacting with customers.
4. **Implicit disutility from earnings uncertainty:** Under variable-pay schemes, drivers may experience costs from unpredictable earnings even if we model utility as linear in expected earnings.

Because we model utility as linear in earnings and interpret β as an effective planning horizon rather than a deep structural time preference parameter (see Section 4.2), the cost parameter C_i absorbs these multiple factors into a single reduced-form measure. This approach is standard in discrete choice models where the researcher observes choices but not the complete set of costs and benefits that agents trade off.

An important implication is that our finding that guaranteed pay reduces switching could operate through multiple channels. If C_i includes a component reflecting disutility from earnings uncertainty, then guaranteed pay effectively lowers the cost of remaining active by reducing this uncertainty. This is observationally equivalent to our specification where guaranteed pay directly affects the flow payoff through the hourly wage term. We cannot separately identify these mechanisms with our data, but both interpretations support the same policy implication: guaranteed pay is cost-effective for retention because it aligns with drivers' preferences for predictable compensation.

For readers interested in structural interpretations, we note that our cost estimates are most directly comparable to the marginal cost of remaining active for an additional epoch (20 minutes), not to the average cost per hour of work including fixed costs. The relatively low magnitude (\$1.66 per hour) is thus consistent with drivers making granular, short-horizon decisions about whether to continue working based primarily on flow costs rather than sunk costs.

A.3. Recovering Driver-Level Cost Indices

This appendix describes how we recover a driver-specific cost index $\hat{C}_i$ that summarizes heterogeneity in the per-epoch cost of work. The model in §3 treats C_i as a time-invariant driver attribute drawn once per driver from a truncated Normal distribution. Our structural estimation in §4 identifies the population parameters $(\hat{\beta}, \hat{\mu}_C, \hat{\sigma}_C)$ by matching aggregate quitting patterns. Here we condition on these estimates and recover a driver-level point estimate $\hat{C}_i$ as a descriptive object.

Inputs and outcomes used. For each driver i, we use the subset of driver-day sessions in which the driver starts on platform A. For each session, we observe the start state (start time and start region) and the session termination outcome (quit time block and quit region, and whether the driver switches from A to B prior to quitting if that indicator is available in our data construction). We denote the collection of outcomes for driver i by $\mathcal{D}_i$.

Second-stage mapping from C to predicted session outcomes. Fix $\hat{\beta}$ and the estimated environment primitives (matching probabilities, destination distributions, and trip durations) used in the structural estimation. For a candidate cost level C on a grid $C \in [\underline{C}, \bar{C}]$, we simulate the model forward from each observed start state in $\mathcal{D}_i$ and compute the model-implied probability of each observed termination outcome.[9]

Let $\widehat{p}(\mathcal{D}_i \mid C, \hat{\beta})$ denote the resulting (simulated) likelihood of observing driver i's session outcomes given cost C.

Driver-level cost index. We recover a driver-level point estimate $\hat{C}_i$ as the posterior mean of C_i under an empirical Bayes prior equal to the estimated population distribution:

$$p(C_i \mid \mathcal{D}_i) \propto p(C_i; \hat{\mu}_C, \hat{\sigma}_C) \cdot \widehat{p}(\mathcal{D}_i \mid C_i, \hat{\beta}), \tag{EC.1}$$

where $p(C_i; \hat{\mu}_C, \hat{\sigma}_C)$ is the truncated Normal prior over $[\underline{C}, \bar{C}]$.

We then summarize each driver's posterior by a single number,

$$\hat{C}_i = \mathbb{E}[C_i \mid \mathcal{D}_i], \tag{EC.2}$$

computed numerically on the same cost grid. Figure 5 plots the histogram of $\{\hat{C}_i\}_i$.

Interpretation. The object $\hat{C}_i$ is a descriptive index that captures persistent differences in drivers' incremental cost of remaining active, bundling operating costs, effort and fatigue, and other opportunity costs as in §3. Because it is computed conditional on $(\hat{\beta}, \hat{\mu}_C, \hat{\sigma}_C)$, it should not be interpreted as a separately identified structural primitive beyond the maintained model.

A.4. Implications of Estimated Cost Heterogeneity

After recovering the cost distribution from our adversarial estimation, we can examine what patterns of behavior the estimated heterogeneity implies. Figures EC.1 and EC.2 show simulated utilization rates and switching probabilities by day of week and time of day, generated by drawing costs from the estimated distribution $\text{TruncNormal}(\hat{\mu}_C, \hat{\sigma}_C^2; 0, 5)$ and simulating forward using the estimated discount factor $\hat{\beta}$.

The simulated patterns reveal how the recovered cost heterogeneity shapes aggregate behavior. Utilization rates peak during midday and afternoon rush hours when guaranteed wages are highest, then decline in late evening as wages fall and drivers with higher costs find it no longer profitable to continue. The gradual decline rather than a sharp drop-off reflects the heterogeneity in C_i: drivers with the highest costs quit first when wages begin to fall, followed by those with moderate costs, while drivers with the lowest costs remain active even during low-wage periods.

Switching probabilities spike sharply at shift boundaries (marked by grey dashed lines), precisely when guaranteed wages change. These spikes occur because drivers reassess their outside options when the value of staying on platform A shifts discontinuously. The magnitude of these spikes varies across the cost distribution: drivers with high costs are more sensitive to wage changes and more likely to switch when wages fall, while drivers with low costs exhibit more

[9] In practice, we approximate these probabilities by Monte Carlo simulation using the same discretization of time and space as the quitting heatmaps.

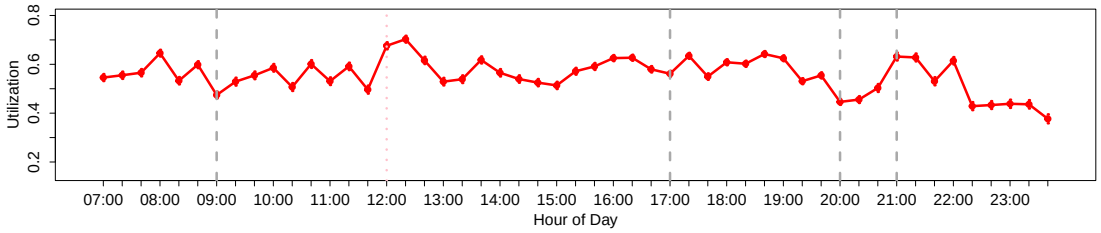

(a) Mondays

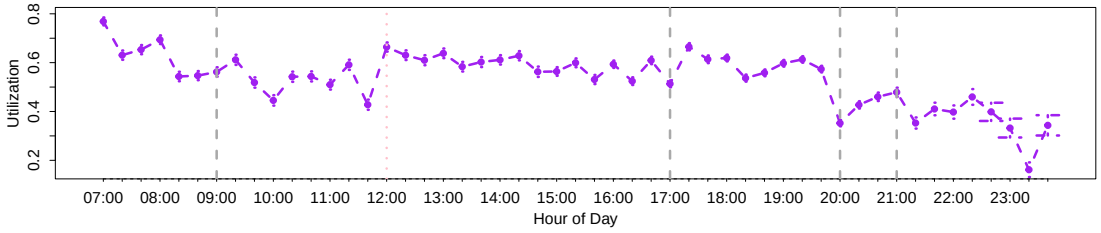

(b) Tuesdays

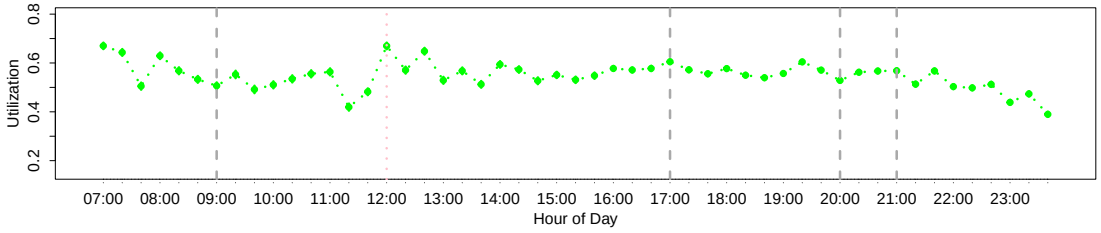

(c) Wednesdays

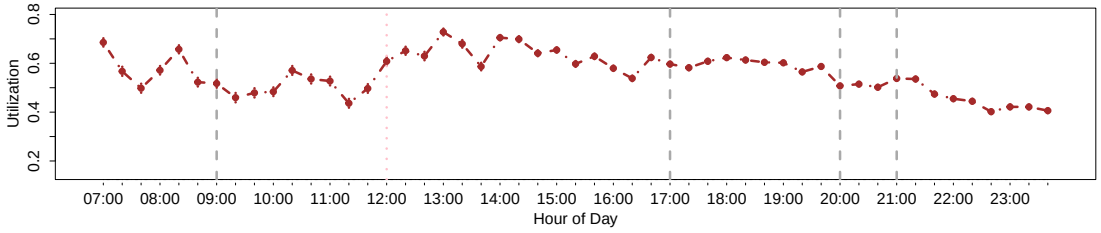

(d) Thursdays

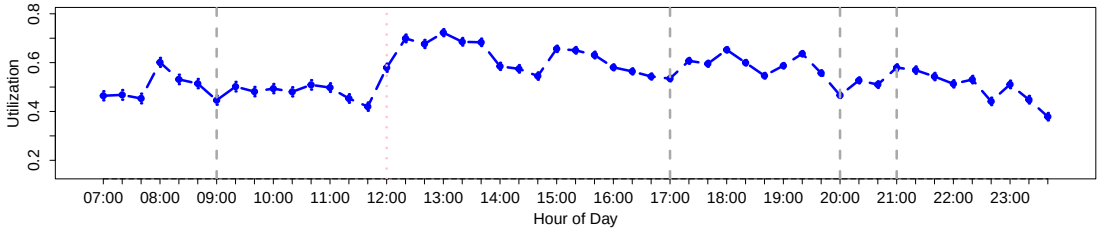

(e) Fridays

Figure EC.1 Simulated utilization rates by day of week and time of day using estimated cost distribution. Patterns generated by drawing $C_i \sim \textbf{TruncNormal}(\hat{\mu}_C, \hat{\sigma}^2_C; 0, 5)$ for each driver and simulating forward with estimated parameters. Grey dashed lines represent shift boundaries; pink dotted line represents noon.

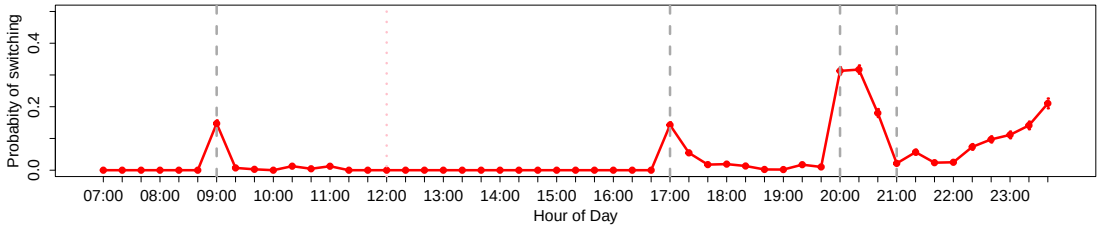

(a) Mondays

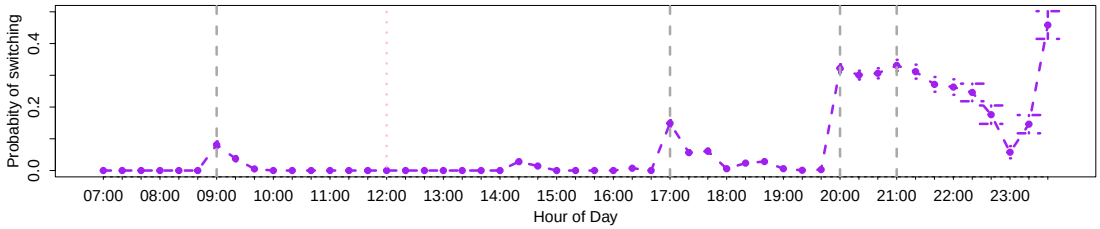

(b) Tuesdays

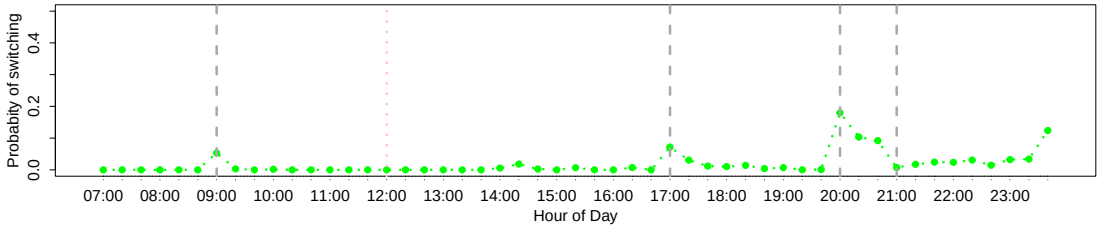

(c) Wednesdays

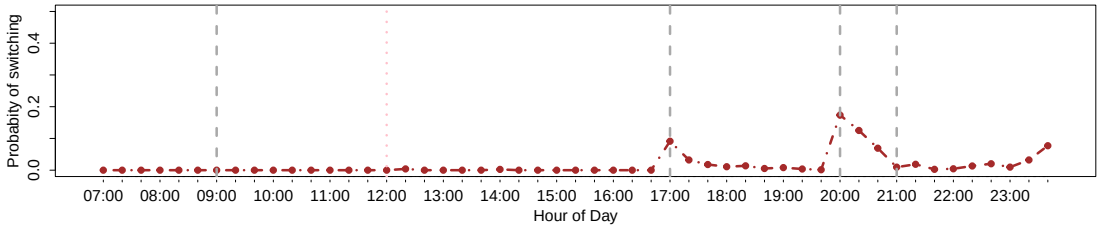

(d) Thursdays

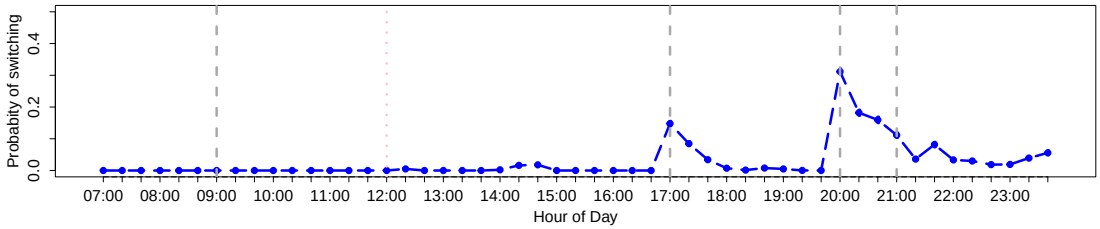

(e) Fridays

Figure EC.2 Simulated switching probabilities by day of week and time of day using estimated cost distribution. Patterns generated by drawing $C_i \sim \text{TruncNormal}(\hat{\mu}_C, \hat{\sigma}_C^2; 0, 5)$ for each driver and simulating forward with estimated parameters. Grey dashed lines represent shift boundaries; pink dotted line represents noon.

stable attachment to platform A. The patterns are consistent across weekdays, with slight variation on Fridays when evening activity extends later.

These simulated patterns demonstrate that the estimated cost distribution, combined with the estimated discount factor, generates economically sensible heterogeneity in driver behavior. Drivers do not respond uniformly to wages and outside options; rather, their responses depend on their individual costs of working. This heterogeneity is central to our policy counterfactuals in §6, where we examine how different pay designs affect drivers differently depending on their position in the cost distribution.

Appendix B: Theoretical Validation

B.1. Consistency of the WGAN-GP Adversarial Estimator

This appendix verifies that our WGAN-GP implementation satisfies the regularity conditions in Kaji et al. (2023), ensuring consistency of the generator estimator.

Overview. Kaji et al. (2023) study adversarial estimators in a general setting where a generator parameter θ is chosen to minimize a discrepancy between real data and model simulations as measured by an optimally trained critic. Our implementation differs in that we impose 1-Lipschitzness on the critic via the WGAN-GP gradient penalty rather than an explicit constraint. We show that under standard regularity assumptions, this penalty-based implementation fits within their framework and delivers consistent estimates.

Problem setup. Consider a generator model $G_\theta(z)$ with parameter $\theta \in \Theta$ and a critic network $D_\phi(x)$ with parameter $\phi \in \Phi$. Let P_{real} denote the true data distribution and P_θ the model distribution induced by G_θ.

In WGAN-GP (Gulrajani et al. 2017), the population penalized objective for the critic, given fixed θ, is:

$$M_\theta^\lambda(D_\phi) = \mathbb{E}_{x\sim P_{\text{real}}}[D_\phi(x)] - \mathbb{E}_{x\sim P_\theta}[D_\phi(x)] - \lambda \mathbb{E}_{\hat{x}}\left[\left(\|\nabla_{\hat{x}} D_\phi(\hat{x})\|_2 - 1\right)^2\right],$$

where $\hat{x} = \alpha x_{\text{real}} + (1-\alpha)x_{\text{fake}}$ with $\alpha \sim \text{Unif}[0,1]$, and $\lambda > 0$ is the gradient-penalty weight.

The population best critic in the network class is:

$$D_\theta^\lambda \in \arg\max_{\phi\in\Phi} M_\theta^\lambda(D_\phi).$$

Let $\mathcal{D}_1$ denote the class of all 1-Lipschitz functions. The ideal (unpenalized) adversarial objective is:

$$M_\theta(D) = \mathbb{E}_{x\sim P_{\text{real}}}[D(x)] - \mathbb{E}_{x\sim P_\theta}[D(x)], \quad D \in \mathcal{D}_1,$$

with value:

$$m(\theta) := \sup_{D\in\mathcal{D}_1} M_\theta(D).$$

This is the Kantorovich-Rubinstein dual representation of the Wasserstein distance between P_{real} and P_θ.

Given data $\{x_i\}_{i=1}^n$ from P_{real} and simulated samples from P_θ, we form empirical analogues and train a critic that approximately maximizes the empirical penalized objective:

$$\hat{D}_{\theta,n} \in \arg\max_{\phi\in\Phi} \hat{M}_{\theta,n}^\lambda(D_\phi).$$

We estimate the generator by:

$$\hat{\theta}_n \in \arg\min_{\theta\in\Theta} \hat{M}_{\theta,n}^\lambda(\hat{D}_{\theta,n}).$$

Consistency result. Let $\theta_0 \in \Theta$ denote the true parameter, so $P_{\text{real}} = P_{\theta_0}$. We establish consistency: $\hat{\theta}_n \xrightarrow{p} \theta_0$.

Step 1: Penalized critic approximates the 1-Lipschitz optimum. Assume: (i) The network class $\{D_\phi : \phi \in \Phi\}$ can approximate any 1-Lipschitz function arbitrarily well (universal approximation). (ii) The penalty weight λ is chosen so empirical optimization remains well-posed. (iii) The penalty is effective: $\|\nabla_x D_\theta^\lambda(x)\|_2 \to 1$ in probability uniformly in θ.

Under these conditions, maximizers D_θ^λ of the penalized problem approximate maximizers over 1-Lipschitz functions, and:

$$\sup_{\theta \in \Theta} |m^\lambda(\theta) - m(\theta)| \to 0,$$

where $m^\lambda(\theta) := \sup_{\phi \in \Phi} M_\theta^\lambda(D_\phi)$.

Step 2: Uniform convergence of empirical objectives. Assume uniform law of large numbers:

$$\sup_{\theta \in \Theta, \phi \in \Phi} |\hat{M}_{\theta,n}^\lambda(D_\phi) - M_\theta^\lambda(D_\phi)| \xrightarrow{p} 0.$$

This follows from empirical process theory given the complexity of the critic class. Because trained critics are approximate maximizers with optimization error $\delta_n \to 0$:

$$\sup_{\theta \in \Theta} |\hat{M}_{\theta,n}^\lambda(\hat{D}_{\theta,n}) - m^\lambda(\theta)| \xrightarrow{p} 0.$$

Step 3: Argmin consistency. Combining Steps 1 and 2:

$$\sup_{\theta \in \Theta} |\hat{M}_{\theta,n}^\lambda(\hat{D}_{\theta,n}) - m(\theta)| \xrightarrow{p} 0.$$

Assume: (a) Θ is compact. (b) $m(\theta)$ is continuous and has unique minimizer at θ_0.

Uniqueness is natural in our setting: P_θ equals P_{real} only at θ_0, so the Wasserstein distance attains its minimum uniquely there. Standard argmin consistency (e.g., Newey and McFadden 1994) implies:

$$\hat{\theta}_n \xrightarrow{p} \theta_0.$$

Conclusion. The use of WGAN-GP with gradient penalty rather than explicit Lipschitz constraint does not alter the consistency argument. The critic class consistently approximates the ideal objective, empirical objectives converge uniformly, and the generator estimator is an argmin of a well-behaved criterion with unique minimizer at the true parameter. Under stated conditions, our WGAN-GP adversarial estimator is consistent.

B.2. Validation on a Toy Problem

This appendix validates our WGAN-GP adversarial estimator on a simple one-dimensional problem where the true data-generating process is known. The exercise verifies that the method can recover distributional parameters and, crucially for our policy counterfactuals, reproduce tail probabilities.

Setup. Let $Y_{\text{real}} \sim \text{TruncNorm}(2, 1.5^2; 0, 5)$ be the true data-generating process (truncated normal with mean 2, variance 1.5^2, support $[0, 5]$). The generator produces synthetic data $Y_{\text{sim}} \sim \text{TruncNorm}(\theta, \sigma^2; 0, 5)$ with free parameters (θ, σ). We initialize at $(\theta, \sigma) = (1, 1)$ and update through adversarial training.

WGAN-GP training. We adopt the Wasserstein GAN with Gradient Penalty framework (Gulrajani et al. 2017) for stability. The critic loss is:

$$L_D = \mathbb{E}_{x \sim P_{\text{fake}}}[D(x)] - \mathbb{E}_{x \sim P_{\text{real}}}[D(x)] + \lambda \mathbb{E}_{\hat{x}}\left[(\|\nabla_{\hat{x}} D(\hat{x})\|_2 - 1)^2\right],$$

where $\hat{x} = \alpha x_{\text{real}} + (1 - \alpha) x_{\text{fake}}$ with $\alpha \sim U(0, 1)$ and $\lambda = 10$.

Configuration. We use a three-layer MLP critic with LeakyReLU and LayerNorm, mini-batch size 128, Adam optimizers (learning rate 10^{-4} for critic, 5×10^{-5} for generator), and train for 3,000 generator iterations with 20 critic updates per generator update.

Evaluation. We focus on tail behavior relevant to our policy counterfactuals. We draw 100 samples from Y_{real} and 100 from Y_{sim} and compute: (i) sample mean and standard deviation, (ii) fraction of observations ≥ 3 (representing drivers whose earnings exceed a threshold).

Results. Table EC.1 compares summary statistics after training. The generated distribution closely matches the real distribution on mean, dispersion, and upper-tail probability. Figure EC.3 plots empirical densities.

Table EC.1 Comparison of real and generated data after WGAN-GP training

Quantity	Real data	Generated data
Mean (μ)	2.1295	2.1254
Standard deviation (σ)	1.0441	1.1315
Fraction ≥ 3	0.240	0.248

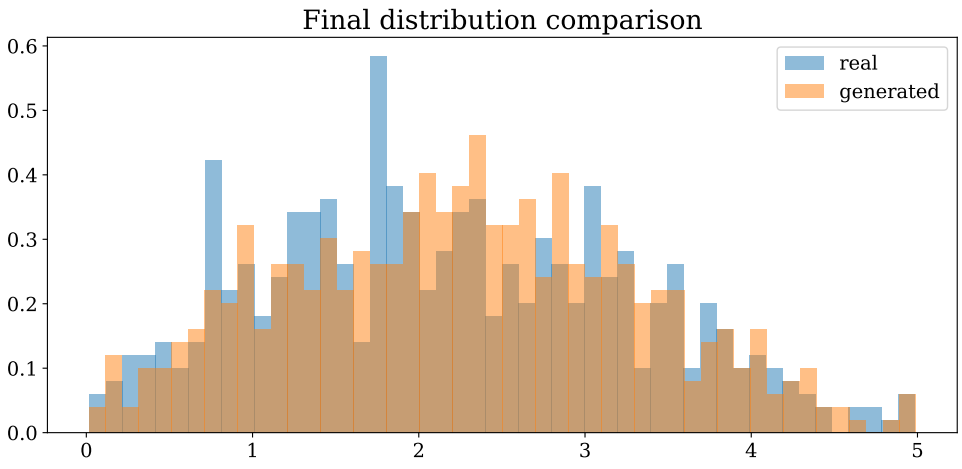

Figure EC.3 Comparison of real and simulated distributions using WGAN-GP

This simple experiment provides additional validation that WGAN-GP can recover distributional parameters and tail probabilities. While a one-dimensional problem cannot guarantee performance in our high-dimensional structural setting, it confirms that the method works as intended when the data-generating process is known.

Appendix C: Computational Implementation

C.1. Pre-Computation of Value Functions

A key computational challenge is that value functions depend on driver-specific cost C_i and common discount factor β, while adversarial estimation requires repeatedly simulating driver trajectories for many candidate values of (μ_C, σ_C, β). Directly resolving dynamic programs for each candidate would be prohibitively costly.

We separate implementation into two stages. First, we pre-estimate environment primitives that do not depend on (μ_C, σ_C, β): matching probabilities R^A_{lt} and R^B_{lt}, trip distributions π^A_{lkt} and π^B_{lkt}, trip durations τ^A_{lk} and τ^B_{lk}, and TLC-based measures of expected trip earnings and supply shortage for platform B. These are estimated using proprietary data from platform A and TLC records (§2) and treated as fixed inputs.

Second, we pre-compute value functions on a grid over cost and discount-factor values. We construct finite grids $\mathcal{G}_C \times \mathcal{G}_\beta$ over the support of C_i and plausible values of β. For platform B, we use 101 cost points ($C \in [0,5]$ with increment 0.05) and 9 discount factors ($\beta \in \{0.8, 0.825, ..., 0.98\}$), computed separately for weekdays and weekends. For platform A, we use a sparser grid (13 cost values, 6 discount factors) and compute driver-date-specific values for each of the 11,109 driver-day pairs in our sample, accounting for the heterogeneous guaranteed wage schedules.

For each grid point $(C^g, \beta^h) \in \mathcal{G}_C \times \mathcal{G}_\beta$, we solve the driver's dynamic programming problem by backward induction using pre-estimated environment primitives. This yields value functions $\{V^A_{lt}(C^g, \beta^h), V^B_{lt}(C^g, \beta^h)\}$ at each state (l,t) for each parameter pair, which we store.

Interpolation. During adversarial estimation, when simulating driver i with drawn cost C_i and candidate β, we approximate value functions by bilinear interpolation from the pre-computed grid. We locate the rectangle in (C, β) space containing (C_i, β) and form weighted averages of the four surrounding grid points. Our grid spacing (0.05 for costs over support $[0,5]$; at most 0.025 for discount factors over $[0.8, 0.98]$) ensures negligible approximation error given typical value function magnitudes in our setting. The fine grid spacing relative to the range of values means that interpolated values closely approximate the exact solutions that would be obtained by solving the dynamic program at (C_i, β) directly.

This interpolation-based approach preserves the richness of the dynamic model while keeping numerical burden manageable. Pre-computation is performed once before estimation begins. Subsequent evaluations during adversarial optimization require only interpolation and simulation, making each iteration computationally tractable.

C.2. Detailed Simulation Procedure

This appendix provides the complete step-by-step procedure for simulating driver trajectories given candidate parameters $\theta = (\beta, \mu_C, \sigma_C)$ and pre-computed environment primitives.

Initialization. For each driver i who worked on day d in the observed data:

Step 1: Draw cost. Draw driver i's cost C_i from TruncNormal(μ_C, σ_C) over support $[0,5]$ using inverse CDF sampling:

$$C_i = \Phi^{-1}\left(\Phi\left(\frac{0-\mu_C}{\sigma_C}\right) + \epsilon_i\left[\Phi\left(\frac{5-\mu_C}{\sigma_C}\right) - \Phi\left(\frac{0-\mu_C}{\sigma_C}\right)\right]\right)\cdot\sigma_C + \mu_C,$$

where $\epsilon_i \sim$ Uniform$[0,1]$ and Φ is the standard normal CDF.

Step 2: Set initial state. Initialize driver i at her observed starting location l_0 and time t_0 from the proprietary data.

Forward simulation. While driver i remains active (has not quit), at each decision epoch t:

Step 3: Compute continuation values. Obtain $V^A_{ilt}(C_i, \beta)$ and $V^B_{ilt}(C_i, \beta)$ by bilinear interpolation over the pre-computed value function grids described in Appendix C.1.

Step 4: Compute option values. Compute the value of each available action:

- If currently on platform A:
  - Value of staying: $V_i(\text{Stay}; A, l, t) + \epsilon^{\text{Stay}}_{ilt}$

— Value of switching: $V_i(\text{Switch}; A, l, t) + \epsilon_{ilt}^{\text{Switch}} = V_i(\text{Stay}; B, l, t) + \epsilon_{ilt}^{\text{Switch}}$

— Value of quitting: $0 + \epsilon_{ilt}^{\text{Quit}}$

- If currently on platform B:

— Value of staying: $V_i(\text{Stay}; B, l, t) + \epsilon_{ilt}^{\text{Stay}}$

— Value of quitting: $0 + \epsilon_{ilt}^{\text{Quit}}$

where $\{\epsilon_{ilt}^{a}\}$ are i.i.d. extreme value shocks drawn for each option.

Step 5: Simulate choice. Driver chooses action a^* that maximizes value:

$$a^* = \arg\max_a \left\{ V_i(a; \cdot, l, t) + \epsilon_{ilt}^{a} \right\}.$$

Step 6: Record quit or continue.

- If a^* = Quit: Record quit time t and location l. Stop simulating this driver.
- If a^* = Switch: Update current platform to B. Continue to Step 7.
- If a^* = Stay: Continue to Step 7.

Step 7: Simulate matching and trip (if staying). If driver chose to stay on her current platform $j \in \{A, B\}$:

- Draw matching outcome: Matched $\sim$ Bernoulli(R_{lt}^{j})
- If matched:

— Draw destination: $k \sim \text{Discrete}(\{\pi_{lkt}^{j}\}_k)$

— Retrieve trip duration: τ_{lk}^{j}

— Advance time: $t \leftarrow t + \tau_{lk}^{j}$

— Update location: $l \leftarrow k$

- If not matched:

— Advance time: $t \leftarrow t + 1$

— Location remains: $l \leftarrow l$

Step 8: Check time limit. If $t \geq$ midnight, driver automatically quits. Record quit time and location. Otherwise, return to Step 3.

Aggregation. After simulating all drivers who worked on day d:

Step 9: Construct heatmap. For each location l and hour h, count the number of drivers who quit at location l during hour h. Normalize by total drivers to obtain:

$$f_{l,h}^{d} = \frac{\text{Number of drivers quitting at } (l, h) \text{ on day } d}{\text{Total drivers working on day } d}.$$

Step 10: Vectorize. Stack $\{f_{l,h}^{d}\}_{l,h}$ into matrix Q_d^{θ} and vectorize to obtain X_d^{θ}.

Step 11: Stack across days. Repeat for all days d in the sample to obtain $\{X_d^{\theta}\}_d$.

This procedure ensures that the simulated distribution of quit times and locations reflects the structural model's predictions given parameters θ, while respecting the constraints imposed by the pre-estimated environment primitives.

C.3. Numerical Gradient Computation

This appendix derives the gradient of the adversarial loss with respect to our structural parameters $\theta = (\beta, \mu_C, \sigma_C)$, which is used for parameter updates in §4.4.

The cross-entropy loss function is:

$$\mathcal{L}(\theta) = -\sum_{i:Y_i=1} \log(\hat{D}(X_i)) - \sum_{i:Y_i=0} \log(1-\hat{D}(X_i)),$$

where $\hat{D}$ is the trained discriminator, X_i are outcome vectors (vectorized quitting heatmaps), and $Y_i \in \{0,1\}$ indicates whether observation i is real (1) or simulated (0).

Our input X has dimension $(D \cdot H) \times L$, where D is the number of days, $H = 17$ hours (7am to midnight), and $L = 20$ NYC regions. Keras automatic differentiation provides $\partial\mathcal{L}/\partial X$. We compute the parameter gradient via the chain rule:

$$\frac{\partial \mathcal{L}}{\partial \theta} = \frac{\partial \mathcal{L}}{\partial X} \cdot \frac{\partial X}{\partial \theta}.$$

We need the Jacobian:

$$\frac{\partial X}{\partial \theta} = \left[\frac{\partial X}{\partial \beta} \quad \frac{\partial X}{\partial \mu_C} \quad \frac{\partial X}{\partial \sigma_C}\right].$$

Structure of X. Each cell $X_{l,h,d}$ records the fraction of drivers who quit at location l during hour h on day d:

$$X_{l,h,d} = \frac{1}{|D_d|} \sum_{i \in D_d} q^i_{l,h,d},$$

where D_d is the set of drivers who worked on day d and $q^i_{l,h,d}$ is driver i's simulated probability of quitting at location l and hour h on day d. Therefore:

$$\frac{\partial X_{l,h,d}}{\partial \theta} = \frac{1}{|D_d|} \sum_{i \in D_d} \frac{\partial q^i_{l,h,d}}{\partial \theta}.$$

Cost sampling and derivatives. For each driver i, we draw cost C_i from TruncNormal(μ_C, σ_C^2) over support $[0,5]$ using inverse CDF sampling. Specifically, we draw $\epsilon_i \sim$ Uniform$[0,1]$ and compute:

$$C_i = \Phi^{-1}\left(\Phi\left(\frac{0-\mu_C}{\sigma_C}\right) + \epsilon_i\left[\Phi\left(\frac{5-\mu_C}{\sigma_C}\right) - \Phi\left(\frac{0-\mu_C}{\sigma_C}\right)\right]\right) \cdot \sigma_C + \mu_C,$$

where Φ is the standard normal CDF. The derivatives of C_i with respect to parameters are:

$$\frac{\partial C_i}{\partial \beta} = 0, \quad \frac{\partial C_i}{\partial \mu_C} = 1, \quad \frac{\partial C_i}{\partial \sigma_C} = \Phi^{-1}\left(\Phi\left(\frac{0-\mu_C}{\sigma_C}\right) + \epsilon_i\left[\Phi\left(\frac{5-\mu_C}{\sigma_C}\right) - \Phi\left(\frac{0-\mu_C}{\sigma_C}\right)\right]\right).$$

Derivatives through bilinear interpolation. In pre-computation, we computed $q^i_{l,h,d}(\beta, C)$ on a grid. During simulation, we obtain $q^i_{l,h,d}(\beta, C_i)$ by bilinear interpolation over the four nearest grid points: (β_1, C_1), (β_1, C_2), (β_2, C_1), (β_2, C_2), where $\beta_1 < \beta < \beta_2$ and $C_1 < C_i < C_2$.

The interpolated value is:

$$\begin{aligned} q^i_{l,h,d}(\beta, C_i) = \frac{1}{(\beta_2-\beta_1)(C_2-C_1)}\Big[& q^i_{l,h,d}(\beta_1, C_1)(\beta_2-\beta)(C_2-C_i) \\ & + q^i_{l,h,d}(\beta_2, C_1)(\beta-\beta_1)(C_2-C_i) \\ & + q^i_{l,h,d}(\beta_1, C_2)(\beta_2-\beta)(C_i-C_1) \\ & + q^i_{l,h,d}(\beta_2, C_2)(\beta-\beta_1)(C_i-C_1)\Big]. \end{aligned}$$

Taking derivatives:

$$\frac{\partial q^i_{l,h,d}(\beta, C_i)}{\partial \beta} = \frac{1}{(\beta_2-\beta_1)(C_2-C_1)}\Big[-q^i_{l,h,d}(\beta_1, C_1)(C_2-C_i) + q^i_{l,h,d}(\beta_2, C_1)(C_2-C_i) \\ - q^i_{l,h,d}(\beta_1, C_2)(C_i-C_1) + q^i_{l,h,d}(\beta_2, C_2)(C_i-C_1)\Big],$$

$$\frac{\partial q^i_{l,h,d}(\beta, C_i)}{\partial \mu_C} = \frac{1}{(\beta_2-\beta_1)(C_2-C_1)}\Big[-q^i_{l,h,d}(\beta_1, C_1)(\beta_2-\beta) - q^i_{l,h,d}(\beta_2, C_1)(\beta-\beta_1) \\ + q^i_{l,h,d}(\beta_1, C_2)(\beta_2-\beta) + q^i_{l,h,d}(\beta_2, C_2)(\beta-\beta_1)\Big],$$

$$\frac{\partial q^i_{l,h,d}(\beta, C_i)}{\partial \sigma_C} = \frac{1}{(\beta_2-\beta_1)(C_2-C_1)}\frac{\partial C_i}{\partial \sigma_C}\Big[-q^i_{l,h,d}(\beta_1, C_1)(\beta_2-\beta) - q^i_{l,h,d}(\beta_2, C_1)(\beta-\beta_1) \\ + q^i_{l,h,d}(\beta_1, C_2)(\beta_2-\beta) + q^i_{l,h,d}(\beta_2, C_2)(\beta-\beta_1)\Big].$$

These gradients enable the parameter updates described in §4.4. The chain rule ensures that changes in parameters (β, μ_C, σ_C) propagate through the cost distribution, through the interpolated quit probabilities, through the aggregate quitting heatmaps, and finally through the discriminator to produce the loss gradient.

C.4. Discriminator Architecture and Training Details

This appendix provides the complete specification of the discriminator network architecture and training procedure used in our adversarial estimation.

Wasserstein GAN with gradient penalty. We implement the discriminator using the Wasserstein GAN with gradient penalty (WGAN-GP) framework (Gulrajani et al. 2017) rather than standard binary cross-entropy loss. WGAN-GP improves training stability by enforcing a Lipschitz constraint on the discriminator through gradient penalties rather than weight clipping. The WGAN-GP loss for the discriminator is:

$$\mathcal{L}_D = \mathbb{E}_{x\sim P_{\text{fake}}}[D(x)] - \mathbb{E}_{x\sim P_{\text{real}}}[D(x)] + \lambda \mathbb{E}_{\hat{x}}\left[(\|\nabla_{\hat{x}} D(\hat{x})\|_2 - 1)^2\right],$$

where $\hat{x} = \alpha x_{\text{real}} + (1-\alpha)x_{\text{fake}}$ with $\alpha \sim \text{Unif}[0,1]$, and we set the gradient penalty coefficient $\lambda = 10$.

Network architecture. We implement the discriminator as a feed-forward neural network with the following architecture:

- **Input layer:** $H \times L = 340$ dimensional vector (vectorized quitting heatmap)
- **Hidden layer 1:** 3-unit dense layer
  - — Batch normalization
  - — Leaky ReLU activation with negative slope 0.2
  - — 40% dropout
- **Hidden layer 2:** 3-unit dense layer
  - — Batch normalization
  - — Leaky ReLU activation with negative slope 0.2
  - — 40% dropout

- **Hidden layer 3:** 3-unit dense layer
  - — Batch normalization
  - — Leaky ReLU activation with negative slope 0.2
  - — No dropout
- **Output layer:** 1-unit dense layer with sigmoid activation producing probability in $[0, 1]$

Rationale for architecture choices. The use of leaky ReLU activation (rather than standard ReLU) prevents dead neurons by allowing small negative gradients, which improves training stability. Batch normalization after each dense layer normalizes activations across the mini-batch, reducing internal covariate shift and accelerating convergence. Dropout with rate 40% randomly zeros 40% of activations during training, which prevents overfitting by forcing the network to learn redundant representations. We apply dropout only to the first two hidden layers, not the third, to allow the final layer to use all available features for classification.

Training procedure. We combine simulated outcomes X^θ with observed outcomes X in each training batch, implementing the WGAN-GP procedure as described above. We use batch size 32 and implement soft labeling to improve stability. The discriminator is trained using the Adam optimizer. We train the discriminator for multiple steps before each generator update to ensure it has learned an accurate classification boundary.

Gradient explosion handling. During training, we monitor gradient magnitudes. When gradients exceed pre-determined thresholds in absolute value, we detect potential instability. In such cases, we save current generator parameters, reinitialize discriminator weights using Glorot uniform initialization, and resume training from the saved generator parameters. This prevents training collapse while preserving progress on the generator side.

Implementation. We implement the discriminator using `keras` with `tensorflow` backend. The complete code specifies:

- Weight initialization: Glorot uniform for dense layers
- Bias initialization: Zeros
- Batch normalization momentum: 0.99
- Batch normalization epsilon: 0.001
- Dropout rate: 0.4 (applied during training only, not during inference)

The discriminator is trained end-to-end using backpropagation. Gradients are computed automatically via `tensorflow`'s automatic differentiation and propagated back through the network to update weights. The trained discriminator provides the loss signal for updating the structural parameters as described in §4.4 and Appendix C.3.

Appendix D: Additional Counterfactual Details

D.1. Pay Design: Additional Figures

D.1.1. Distribution of Hours and Trips Figure EC.4 shows the full distribution of daily hours worked and trips completed across pay policies. These distributions complement the weekday-level patterns in Figure 8 by showing how outcomes vary across the driver population. Red dots mark mean values; grey dashed lines mark the guaranteed-pay baseline.

The distributions confirm that guaranteed pay produces higher median hours and trips than pay-per-work at the equivalent rate (1×). The variance in outcomes is similar across policies, suggesting the difference in means arises from a systematic shift in behavior rather than from changes in the composition of workers who remain active.

Figure EC.4 Distribution of hours and trips: guaranteed pay versus pay-per-work

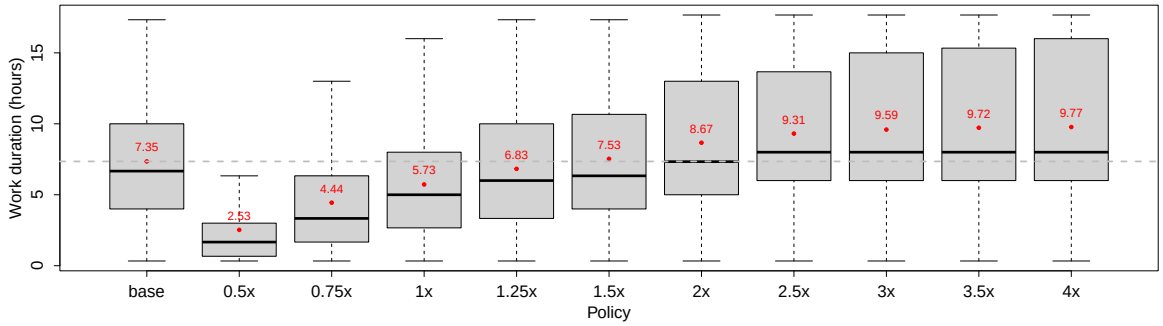

(a) Daily hours

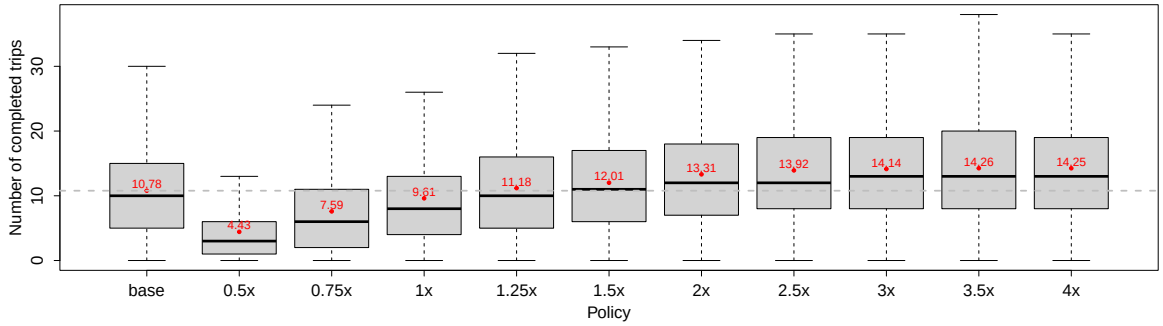

(b) Trips

Note: Red dots are means; grey dashed lines are guaranteed-pay baseline. "·×" denotes per-trip rate relative to equivalent benchmark.

D.1.2. Multihoming Patterns by Weekday Figure EC.5 shows how driver multihoming varies across weekdays for mostly-switchers and always-switchers. These granular patterns complement the aggregate results in Figure 9.

Figure EC.5 Driver multihoming by weekday: guaranteed pay versus pay-per-work

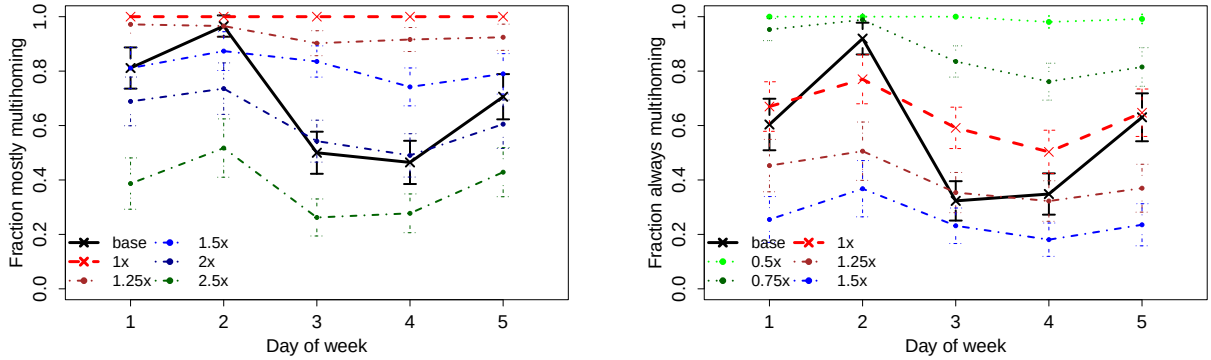

(a) Mostly-switchers

(b) Always-switchers

Note: "·×" denotes per-trip rate relative to equivalent benchmark. Weekdays: 1=Monday,...,5=Friday.

The patterns are consistent across weekdays: pay-per-work at the equivalent rate (1×) produces higher multihoming than guaranteed pay, and substantial per-trip premiums (1.5×–2×) are needed to reduce multihoming back to baseline levels. The consistency suggests our results are not driven by specific day-of-week demand patterns.

D.2. NYC Minimum-Wage Validation: Scope and Limitations

This appendix provides additional context on the NYC minimum-wage validation exercise in §6.3 and discusses important limitations that affect interpretation of the results.

D.2.1. Timing gap between estimation and validation. Our structural model is estimated using data from July 2017, while the minimum-wage policy we use for validation was implemented in early 2019, creating an 18-month gap. During this period, several aspects of the NYC ride-hailing market evolved:

Driver composition. The pool of active drivers changed as new workers entered the market and experienced workers exited. Entry patterns may have shifted following the city's August 2018 decision to cap the total number of for-hire vehicle licenses (Fitzsimmons 2018), which limited the supply of new entrants and potentially changed the composition of active drivers toward those with stronger attachment to ride-hailing work.

Platform technologies. Matching algorithms, pricing systems, and driver interfaces improved over this period as platforms continued to invest in technology. Such improvements could affect both the quality of matches and drivers' ability to multihome efficiently between platforms.

Demand patterns. Overall ride-hailing demand in NYC grew substantially between 2017 and 2019, though growth rates decelerated (Rosaia 2025). Changes in demand levels and spatial-temporal patterns could affect the relative attractiveness of different platforms.

Wage levels. Both guaranteed wages on platform A and per-trip rates on platform B adjusted over time in response to market conditions and driver supply. Our validation exercise holds the pre-policy wage differential constant, which may not reflect actual market dynamics.

We maintain that preference parameters (β, μ_C, σ_C) remain stable over this 18-month horizon. This assumption is more plausible than long-run stability: preferences over pay timing and work effort are likely more stable than market structure. However, if marginal drivers in 2019 differed systematically from those in 2017 (e.g., if remaining drivers after the license cap were more committed), our preference estimates may not fully capture 2019 behavior.

D.2.2. Comparison with Empirical Evidence. Table 2 compares our model predictions with empirical estimates from Koustas et al. (2020) and An et al. (2025). We highlight three points:

Directional consistency. All three analyses (our model and both empirical studies) find that posted wages rise but effective earnings remain flat or fall, driven by reductions in work hours or increases in idle time. This qualitative agreement suggests the myopia mechanism (drivers respond quickly to higher wages without fully anticipating congestion) operates in practice.

Quantitative differences. Our model predicts a 3.5% earnings decline for drivers starting on the exempt platform, while Koustas et al. (2020) finds a 5.4% decline in weekly earnings market-wide and An et al. (2025) finds a statistically insignificant 1.2% decline in monthly earnings. These differences likely reflect: (i) the different enforcement regimes, (ii) the timing gap between our estimation sample and the policy implementation, and (iii) differences in outcome definitions (daily vs. weekly vs. monthly; partial vs. full sample).

Mechanisms. Koustas et al. (2020) documents that platforms responded by actively rationing driver access during low-demand periods, logging drivers off or limiting when they could log on. Our model does not explicitly include platform rationing decisions but captures congestion through increased idle time: drivers remain online but wait longer between trips. Both mechanisms produce similar outcomes, labor supply exceeds demand and drivers work less or earn less despite higher posted rates, but operate through different margins. The fact that our model, which omits active rationing, still predicts earnings declines suggests that drivers' own myopic reallocation decisions are sufficient to generate congestion even before platforms adjust access policies.

D.2.3. Interpretation as Mechanism Validation. Given these limitations, we interpret Section 6.3 as a partial validation that tests whether the model captures the behavioral mechanism: myopic drivers respond to higher posted wages, creating congestion that offsets earnings gains, rather than as a precise quantitative forecast. The qualitative agreement between model predictions and empirical evidence despite substantial differences in setting, timing, and enforcement regime provides support for the core behavioral assumptions (substantial myopia, cost heterogeneity) that drive our counterfactual analyses.

For readers interested in precise quantitative predictions of specific policies, we emphasize that such predictions would require: (i) estimation on data closer in time to the policy implementation, (ii) explicit modeling of platform responses such as access rationing or dynamic pricing, and (iii) incorporating general equilibrium effects through demand elasticities. Our analysis abstracts from these factors to isolate the worker-side behavioral response, which is the focus of our study.

D.3. NYC Minimum-Wage Validation: Hypothetical Scenarios

§6.3 examines the actual 2019 implementation, where the minimum-wage rule applied to per-trip platform B but exempted guaranteed-pay platform A. This appendix explores two hypothetical scenarios to understand how enforcement scope affects congestion and earnings when both platforms operate in the same market.

D.3.1. Scenario design. Beyond the pre-2019 baseline (no rule) and actual 2019 implementation (rule on per-trip competitor only), we simulate:

(c) Guaranteed-pay platform only (hypothetical). The rule applies to the focal platform that pays guaranteed hourly wages; the per-trip competitor is exempt.

(d) Universal enforcement (hypothetical). The rule applies to both platforms.

In scenario (c), we adjust the guaranteed hourly rate w_{it} to meet the \$17.22 minimum. In scenario (d), we adjust both the guaranteed rate and the per-trip rate to meet the minimum on their respective platforms. All scenarios hold demand and fares fixed.

Important caveat. These scenarios are purely hypothetical and cannot be directly compared to empirical evidence. The actual NYC policy exempted guaranteed-pay platforms, and no empirical study has evaluated what would have happened under alternative enforcement regimes. These simulations illustrate how wage floors interact with different pay structures, but should not be interpreted as forecasts of what would occur in practice.

D.3.2. Results. Table EC.2 reports outcomes across all four scenarios.

Table EC.2 NYC minimum-wage rule: full set of scenarios

Outcome (% change)	No rule	Per-trip only	Guaranteed only	Universal
Driver earnings	0.0	−3.5	+3.0	−1.2
Idle time	0.0	+2.1	+3.3	+7.0

Notes: Percentage changes relative to pre-2019 baseline. "Per-trip only" reflects actual 2019 enforcement. "Guaranteed only" and "Universal" are hypothetical scenarios with no empirical counterpart. Demand and fares held fixed.

Enforcement on guaranteed-pay platform only. When the rule applies only to the guaranteed-pay platform (scenario c), driver earnings rise 3.0% but idle time rises 3.3%. This differs from the per-trip-only case. Guaranteed pay already provides hourly compensation, so the minimum acts more like a traditional employment wage floor. Drivers don't face trip-matching uncertainty that dilutes per-trip minimums. The guarantee directly raises pay without requiring completed trips.

However, idle time still rises because the higher guaranteed rate attracts more drivers to platform A or keeps existing drivers online longer. Some of this additional supply cannot be productively absorbed, leading to more time waiting for trip assignments. The net effect on earnings is positive but modest once congestion is accounted for.

Universal enforcement. Under universal enforcement (scenario d), both platforms must meet the minimum. Driver earnings fall 1.2% and idle time rises 7.0%; the largest idle-time increase across all scenarios. The earnings effect is ambiguous: the rule raises posted rates on both platforms, but system-wide supply increases substantially. More drivers compete for the same fixed demand.

The per-trip platform still experiences matching friction (earnings diluted by waiting). The guaranteed-pay platform pays more drivers to be online even when underutilized. The result is high idle time without commensurate earnings gains. This illustrates that broader enforcement does not simply combine the benefits of targeting each platform separately; it can amplify congestion problems.

Comparison across scenarios. The same nominal rule has different effects depending on which pay schemes it targets:

- Per-trip enforcement (actual): Raises posted rates but congestion offsets gains (−3.5% earnings, +2.1% idle time)
- Guaranteed-pay enforcement (hypothetical): More effective at raising earnings but still increases congestion (+3.0% earnings, +3.3% idle time)
- Universal enforcement (hypothetical): Amplifies idle time without resolving earnings ambiguity (−1.2% earnings, +7.0% idle time)

D.3.3. Implications for policy design These scenarios illustrate that minimum-wage rules in gig markets interact differently with different pay structures. Per-trip minimums face dilution through matching frictions. Guaranteed-pay minimums are more effective at raising earnings but still create congestion. Universal enforcement does not automatically improve outcomes; it can compound congestion problems.

Three design principles emerge. First, wage floors should be paired with congestion-management tools: caps on active drivers, priority scheduling during low-demand periods, or dynamic pricing. Without such tools, wage floors

redistribute idle time more than they raise welfare. Second, regulators should account for pay structure differences when setting floors. A uniform hourly minimum translates differently across per-trip and guaranteed-pay schemes. Third, broader enforcement is not automatically better. Universal floors can amplify congestion without proportional welfare gains.

These scenarios are illustrative only. We do not observe what actually happened under guaranteed-only or universal enforcement, so these predictions cannot be validated. They demonstrate that our model generates sensible comparative statics: more enforcement → more congestion, guaranteed-pay enforcement → more effective earnings gains than per-trip enforcement. Whether the precise magnitudes would occur in practice depends on platform responses (access rationing, surge pricing) and demand elasticities that we hold fixed.

References for the E-Companion

An Y, Garin A, Kovak B (2025) Delivering higher pay? the impacts of a task-level pay standard in the gig economy .

Fitzsimmons EG (2018) Uber hit with cap as new york city takes lead in crackdown. URL https://www.nytimes.com/2018/08/08/nyregion/uber-vote-city-council-cap.html.

Gulrajani I, Ahmed F, Arjovsky M, Dumoulin V, Courville AC (2017) Improved training of wasserstein gans. *Advances in neural information processing systems* 30.

Hunter H (2014) Owning and operating your vehicle just got a little cheaper according to aaa's 2014 'your driving costs' study. *AAA NewsRoom* .

Kaji T, Manresa E, Pouliot G (2023) An adversarial approach to structural estimation. *Econometrica* 91(6):2041–2063.

Koustas D, Parrott JA, Reich M (2020) New york city's gig driver pay standard: Effects on drivers, passengers, and the companies .

New York City Department of Consumer and Worker Protection (2022) Minimum pay rate for app-based restaurant delivery workers. Technical report, New York City Department of Consumer and Worker Protection, New York, NY, URL https://www.nyc.gov/assets/dca/downloads/pdf/workers/Delivery-Worker-Study-November-2022.pdf, accessed January 2025.

Newey WK, McFadden D (1994) Large sample estimation and hypothesis testing. *Handbook of econometrics* 4:2111–2245.

Rosaia N (2025) Competing platforms and transport equilibrium. *Econometrica* 93(6):2235–2271.